**IOSUD – „LOWER DANUBE" UNIVERSITY GALAȚI**

**PhD School Engineering Sciences**

UNIVERSITAS

GALATIENSIS

# CONTRIBUTIONS CONCERNING THE ENERGY EFFICIENCY OF NAVAL PROPULSION ELECTRICAL SYSTEMS

**PhD THESIS SUMMARY**

**PhD**

**Gabriel Frangopol**

**Scientific Leader**:                    Prof univ. Emeritus Dr.Eng. Emil Mina Roșu,
                                                     "Lower Danube" University, Galați

**Serie I 3: Electrical Engineering  Nr. 2**

**GALAȚI - 2019**

# INTRODUCTION

## 1.1 UPDATE OF THE FIELD AND MOTIVATION OF RESEARCH

The first electric-powered vessel was launched to the water in 1903 as an oil tanker for the Caspian Sea and the Volga River by the Nobel Petroleum Company. The ship was also revolutionary in that the drive of the electric generator used a diesel engine, replacing the classic solution of that time, steam engine. The arming of new electric powered vessels evolved very slowly until the 90s, around 200 a year, especially icebreakers and dredges, so that after these years the development would become exponential, reaching in 2013 an order of 1750 new ships, of which 199 could be delivered that year. The annual increase of the number of ships with electric propulsion is three times greater than that of the classic ships. The growth trend is not short-term, but it is certain and it is due to several factors. The classic solution, slow, semi-fast or fast diesel engine and fixed pitch propeller, FPP, has certain and well-known disadvantages: the need for a high power mechanical reducer to match the propeller's rotational speed with that of the internal combustion engine; the impossibility of obtaining a specific minimum fuel consumption, optimally, in a wide range of load and speed; the speed adjustment of the ship can be achieved only under the conditions of the total efficiency sacrifice. Major progress has been made by introducing the controllable pitch propeller, CPP, which combines the two rotational speeds so that the primary engine operates in the area of maximum efficiency. The solution allows for the implementation of advanced control, with two command sizes available: propeller pitch and fuel consumption.

The factors that have contributed to the development of electric propulsion fall into two categories: technological developments in related fields; the need to increase the performance of ships; new technologies and applications in the field.

A decisive contribution is provided by power electronics and adjustable electric drive systems. Thus static converters are currently available a.c./a.c. și a.c./d.c. up to powers of the order of tens of MW, covering the power supply for any type and size of ship. The achievable adjustable drive systems, static converters and suitable electric motors are characterized by high efficiency, very good dynamics, reduced gauges and advanced control techniques. The adjustment possibilities are appreciable, being able to independently change the angular speed, torque and power, under the conditions of a higher efficiency. All adjustments are made at the electric motor level, with fixed pitch propellers.

The second important technological breakthrough was the introduction of electric propulsion with AZI-PODs and AZIMUTH-THRUSTERS, which offers superior maneuverability, the possibility of better control of energy efficiency and high navigation performance.

In the development of electric propulsion, an important contribution was brought by the demands imposed by the technologies of offshore exploration and exploitation of oil and gas, the electric propulsion being the most suitable for such applications. The electric propulsion with azipods and azimuth thrusters allowed the development of a new type of control called dynamic positioning, DYNAMIC POSITIONING.

There are also a number of applications that by electric propulsion better solve the technological requirements. Thus, during an offshore operation the auxiliary vessels, the oil pick-up tanks, the service vessels, etc., have to maintain their dynamic position towards the platform even in the event of major storms. Using electric propulsion with today's bridges and dynamic positioning, the problem gets a high-performance and acceptable cost solution. Icebreakers and dredgers, depending on the specific situation, require simultaneous adjustment of torque and speed, easy to obtain in the case of electric propulsion with azi-pods. It also decreases the maximum power required for propulsion as a result of better use of torque-speed availability. For cruise ships, the main requirement is to create a useful space, cabins, common spaces and promenades as large as possible, but also a microclimate, efficient and comfortable air conditioning. The practice shows that the use of electric propulsion, through its small technical spaces, ensures an increased level of comfort and a good use of the spaces available on the ship for passengers.

Last but not least, the price of crude oil and / or gas used comes into the equation. Electric propulsion costs are generally higher than conventional propulsion, but the first one offers clear possibilities for optimizing fuel consumption through adequate control structures.

If top-of-the-line applications, such as dynamic positioning in the oil industry, docks and icebreakers or cruise ships, are complex systems that envisage an optimal production and distribution of electricity aboard the ship, freight ships with electric propulsion have been developed less, using simple schemes, low level automation and paying little attention to the problems regarding energy quality, power losses in the own energy system and the management of reactive and deforming power regimes. Therefore, in the area of classical cargoes, techniques must be developed to compensate for the reactive and deforming powers required by converters and electric motors by active, passive or hybrid filtration. The use of the active derivative power filter, which occupies an increasingly important place in the technique of adjustable electric drives, with original control, indirect control, has been studied, modeled and validated by numerical simulation.

Naval electric propulsion is in fact an electric drive system with some structural and functional features that we highlight:

- Great powers, on the order of megawatts,

- Low rotational speeds to avoid an important and low efficiency mechanical gearbox;

- Adjustable drive, with wide speed control;

- Reversible drive with the possibility of recovering energy from braking periods, preferably without mechanical inverter;

- The ship and the propeller, the propeller make up a strong nonlinear system, so its dynamic modeling is difficult;

- The propeller, given the wide-range speed control, is of the fixed-step type, FPP;

- Given the limited power of the power station serving the ship, the ship's energy system, measures are needed to compensate for reactive power and reduce the deforming regime driven by the drive converter.

Moreover, in this report, only the energetic aspects generated by the converter-drive motor unit at the level of reactive and deforming powers are analyzed and for the case of a general purpose ship, a cargo ship. As an actuation system, it was opted for the analysis of two types more commonly used: AC motor. and SCR thyristor network converter; with three phase induction motor and cycloconverter. These two variants perform the conversion of electricity into a safe step, as opposed to the PWM synchronous converters and inverters, in which the conversion takes place in two steps with appreciable reduction in the conversion efficiency and increase in power electronics losses.

The experimental results, obtained by numerical simulation, confirm that such an analysis was necessary and that the active, passive and hybrid filtrations are useful and can be structured and applied, relatively easily, on any cargo ship.

## 1.2  STRUCTURE OF THE PHD THESIS

The PhD thesis is structured on 9 chapters, with bibliography specific to each chapter.

In Chapter 1, Introduction, the actuality and the theoretical importance of the research field addressed as well as the possible applications resulting from the developed research are argued.

Chapter 2 is entirely devoted to the presentation of the current state of naval electric propulsion. After a brief history of the electric propulsion, the dynamic drives with dynamic positioning specific to the offshore oil industry are reviewed, as well as other applications such as docks, icebreakers and cruise ships. It also presents the classification of electric propulsions in the energy system of ships and develops the problems of reactive and deforming regimes. Finally, there are recent approaches in the field such as switching to distribution in c.c. , DC Grid.

In chapter 3 we analyze two of the sources, converters, dedicated for the electric drives of the propeller: converters c.a. - c.c. with SCR thyristors and cycloconverters c.a. - c.a. The first system studies the operation, the properties and the SIMULINK models of the high power converters with 6 and 12 pulses. For the same purpose, the analysis is developed for the 6-pulse cycloconvertor. Regarding the command of the cycloconvertor, since there are no unified systems in the literature, an original sinusoidal command was devised, which gave satisfactory results in the simulation programs. At the end of the chapter, experimental data obtained by simulating the original SIMULINK models are presented. The rich graphic material confirms the theoretical hypotheses from which it started, validating the models for future uses, including the structuring of a global input-output model. Considerations are also made, based on the graphs presented, of the magnitude and effects of the harmonic and reactive regimes.

The modeling and simulation of the ship is developed in Chapter 4. An analytical model for the ship is taken from the literature, which accurately describes the stationary states, but does not guarantee the accuracy of the dynamic regimes. The main problem is generated by the model of the ship, which, as mentioned above, is strongly nonlinear, depending on several constructive and functional parameters. Starting from this model and approximating by numerical interpolation the functional equations of the ship, a quasi-linear model has been designed that characterizes the precise regimes and the dynamic regimes. The model was validated by simulation in SIMULINK. At the end of the chapter, an analysis

is made of the two variants of propeller: fixed pitch propeller, FPP, and adjustable pitch propeller, CPP. The analysis considers the conversion efficiency in the FPP and electric drive variant.

Chapter 5 is devoted to the automatic control of the actuation of the ship with a DC motor. at constant and / or variable flow. Conventional automation is used for rapid processes, cascade adjustment, in order of the size of the process time constants. The results are also obtained by numerical simulation. For a better use of the electric motor in the acceleration intervals from rest to speed, an original method of mixed control, constant and variable flow is proposed, which improves the dynamic properties, reducing the speed of reaching the speed.

Chapter 6 is dedicated to drive by three-phase induction machine and cycloconvertor using the d / q model with orientation following the rotor magnetic field. All the cascade regulation is used, decoupling the two adjustment channels: U / f=const. and U=const, f=var. The results are obtained by numerical simulation in the SIMULINK environment. And here, as with driving in DC, a new type of control is developed which shortens the duration of dynamic ship acceleration regimes.

Chapters 7 and 8 are dedicated to the stationary regime energy analysis, highlighting the harmonic and reactive regime generated by the converter, network rectifier with SCR thyristors for operating in c.c. and cycloconverter for c.a. An efficient method of reducing the harmonic and reactive regime, an active power filter with indirect control, is proposed and developed. The efficiency of placing the active filter in various topologies and order configurations is studied. Details on the sizing of the active filter and related commands are given. It also presents results obtained by numerical simulation both in terms of the effect of the active filter in steady state and in dynamic regime.

Chapter 9 presents the general conclusions regarding the research carried out, the implications that result from the practical application and which future directions of development can be seen. Also in the chapter is presented a list of the original contributions developed.

## 2.2. TYPE OF SHIPS

Electric powered vessels are used for high performance applications required by modern technologies such as: marine drilling rigs and platforms; oil extraction, production, storage and unloading vessels, FPSO's; Shuttle vessels used to bring crude extracted from platforms to shore; service vessels; cruise ships; ice breakers; dredging vessels.

All these vessels are characterized by their own electrical system of important power, drives with azipods and azimuth thrusters, dynamic positioning, exemplified by the electrical scheme for a marine drilling rig. Fig. 2.3. The power generation module on board the ship usually has between 30 and 40 MW installed power. The drilling vessels usually have six thrusters while the drilling rigs have eight thrusters, each with a rated power of 3-6 MW. Drilling devices and thrusters are the main consumers. The load varies substantially depending on the weather conditions and the way of the drilling process. An automation system is required to ensure the operation of the power plant under maximum load conditions.
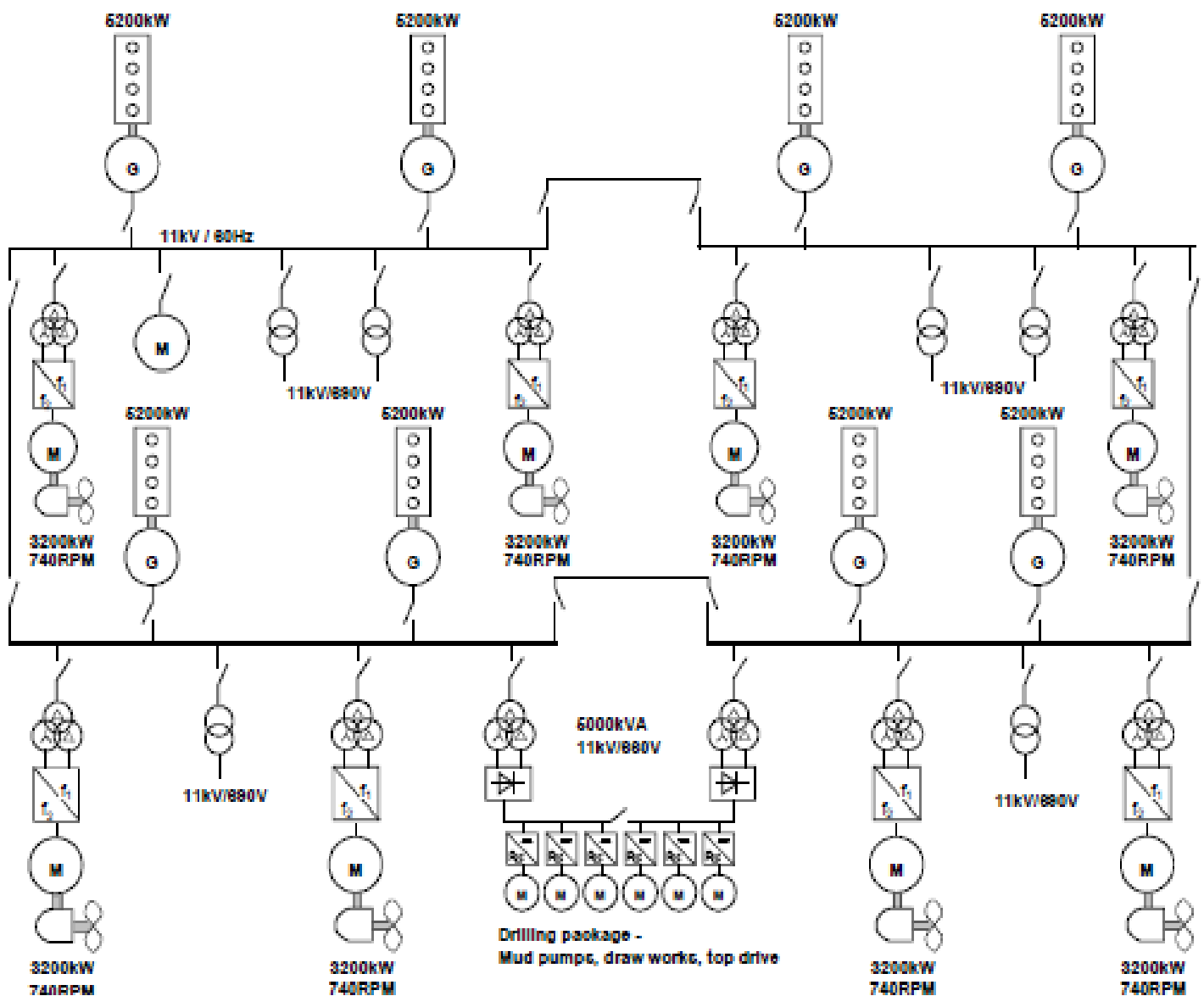
Fig. 2.3. Marine Drilling Rig/Platform

Most of these ships have the classic system of electricity production, Diesel group - synchronous generator. Quite recently, the so-called D.C. was launched. grid, that is, the transformation of the classical force network from c.a. in one in c.c. The first advantage is to reduce the number of non-controlled rectifiers needed for the inverters, as well as the necessary filtering. Only the high power rectifiers on the generators remain, which are cheaper. Secondly, certain possibilities of recovering the braking energy are created through a storage element, ES, a battery of batteries. Another advantage is the easy acquisition of unconventional, photovoltaic or wind energy, available in the work area through the system noted with FC.

The idea from which it started is that the production and distribution equipments are over-dimensioned in order to take over the peaks, while on a functional cycle the load varies greatly. Thus

for a supply platform ship a cycle looks as follows: 35% of time dynamic positioning, characterized by maximum load; 25% heating and transfer; 15% stand by; 25% in port. In the dynamic positioning regime about 13% of the total energy conveyed is in fact energy recovered through converters and motors operating as generators. This energy can be stored, the solution adopted being the accumulator batteries. The result is a hybrid solution whose efficiency is 30% of the total energy.

# CONVERTERS FOR NAVAL ELECTRIC PROPULSION SYSTEMS

## 3.1. CONVERTERS AC – DC

In the case of using c.c. For the propulsion of the naval propeller, the most suitable converters for power supply are the rectifiers ordered with SCR thyristors, which are available at high and very high powers, up to tens of MW, and ensure the continuous and wide adjustment of the engine speed. The most favorable schemes used are the 6-pulse converter in three-phase bridge and the 12-pulse converters, the serial diagram, Fig. 3.1. or parralel.
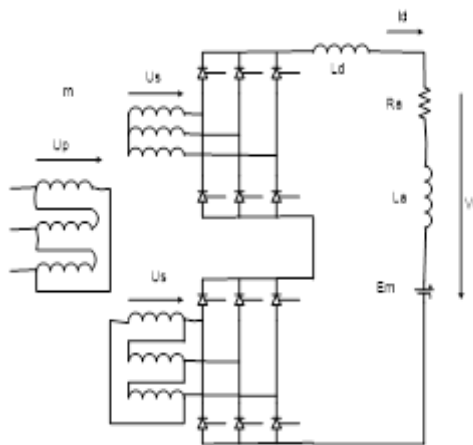


Fig. 3.1. 12-pulse bridge converter, series diagram

The d.c. is modeled by electromotive voltage Em, the parameters of the rotor circuit Ra and La and Ld the inductance of filtration. The transformer m is for adapting the network voltage with that of the motor in Dy connection which cancels the harmonics multiple of 3 of the current injected by the converter through the transformer in the network. The main advantages of the 12 series / bypass pulse scheme are: the reduction of the voltage required in the secondary of the transformer in half and of the spectrum of current harmonics injected into the network at

$$h = 12.k \pm 1 \qquad (3.9)$$

## 2.3. FREQUENCY CONVERTERS AC – AC CYCLOCONVERTERS

Naturally switched frequency converters are alternating - alternating converters whose purpose is to obtain different voltages and frequencies relative to the input voltages at the input. They have a relatively wide range of applicability in the technique, especially for drives with three-phase induction

or synchronous machines of high and very high power due to the use of semiconductor devices with the highest capacity in current and voltage, SCR thyristors.

The principle scheme on a phase of a cycloconverter with 6 pulses in the deck is shown in Fig. 3.9. Essentially, it consists of 2 controlled AC-DC converters, group I and II, mounted antiparallel and forming an AC-DC converter of 4 quadrants. The connection is achieved by the Lf inductivities with a role to limit the movement currents between the two converters, characteristics of the scheme. If the control angles of the two groups are $\alpha_I$, respectively $\alpha_{II}$, fulfilling the condition of the

$$\alpha_I + \alpha_{II} = 180° \qquad (3.21)$$

Then the average tension at the exit of the two groups is calculated:

$$U_{d1} = U_{d0} \cos \alpha_I,$$
$$U_{d2} = U_{d0} \cos \alpha_{II} \qquad (3.22)$$

resulting

$$U_{d1} = -U_{d2} \qquad (3.23)$$

That is, between the two converters does not close a continuous current. Instead, as a result of differences in instantaneous sizes, alternative currents, known as movement currents, appear. To obtain alternative tension at the output of the form

$$u_e(t) = \sqrt{2}U_e \sin\omega_e t \qquad (3.24)$$

The condition shall be required:

$$U_{d1} = -U_{d2} = U_{d0} \cos\alpha_I = \sqrt{2}U_e \sin\omega_e t \qquad (3.25)$$

Where the values of the command angles result:

$$\cos \alpha_I = \frac{\sqrt{2}U_e}{U_{do}} \sin \omega_e t$$

$$\cos \alpha_{II} = -\frac{\sqrt{2}U_e}{U_{do}} \sin \omega_e t \qquad (3.26)$$

The control of the Cycloconverter has the variable amplitude after the amplitude of the desired voltage at the output, and the frequency after pulsation:

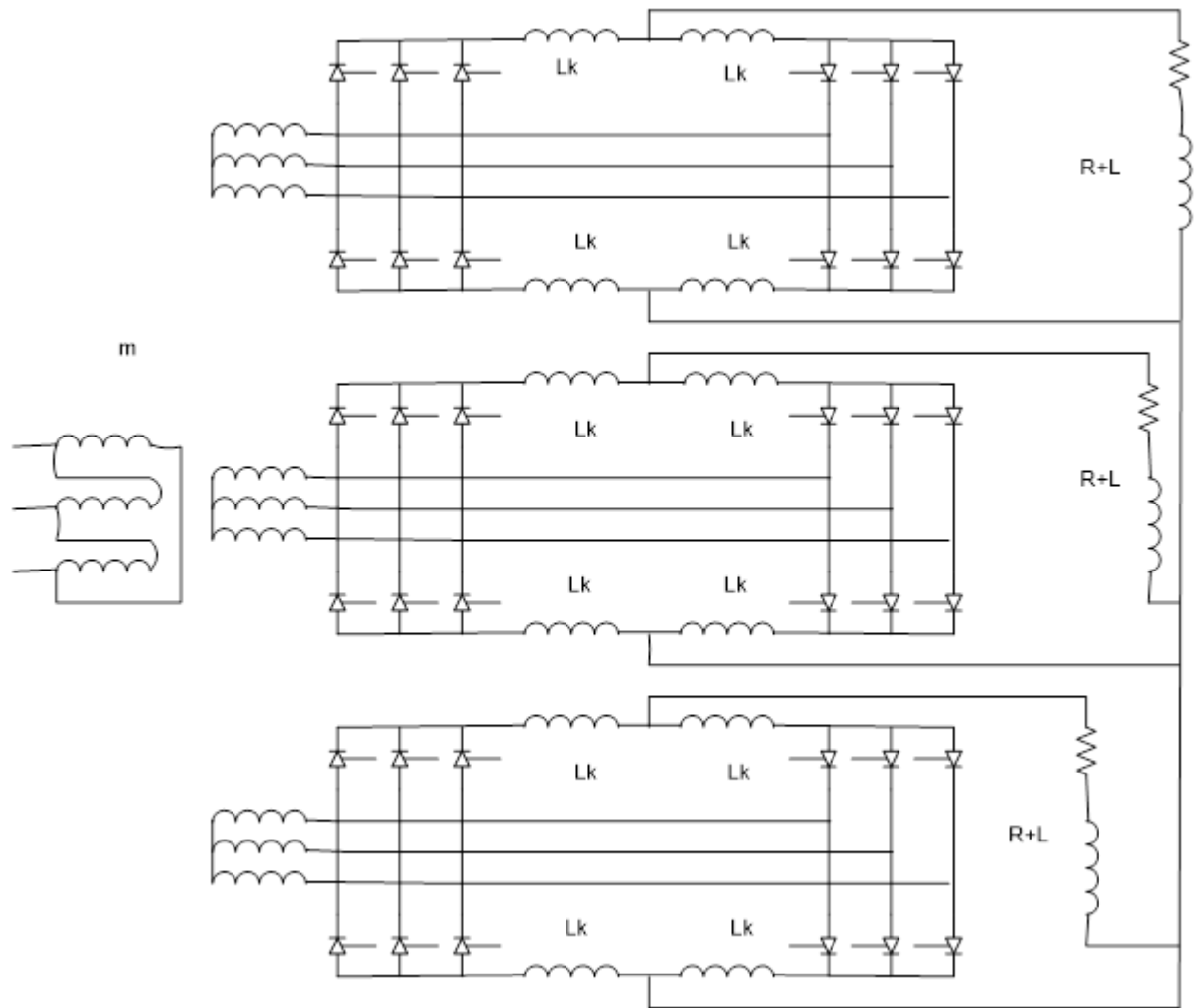$$\omega_e = 2.\pi.f_e \qquad (3.27)$$
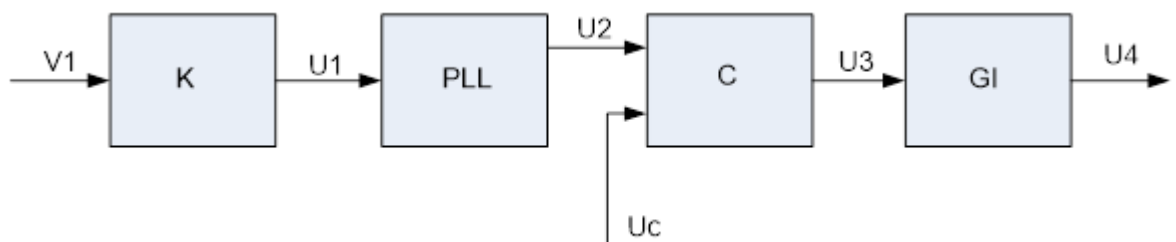
Fig. 3.9 – Cycloconverter with 6 pulses.



Fig. 3.13 – Command channel for a thyristor.

In Fig. 3.13. A command channel is presented for a thyristor, where PLL is the stage-riding block, C comparator, GI pulse generator, and K, Amplitude modulation.

# 4. MODELING AND SIMULATION OF THE SHIP

## 4.1. SHIP MODELING

The model was drawn up with the following assumptions: steady-speed March; Do not interest dynamic ship acceleration or braking regimes as they have an insignificant share in total energy consumption for movement between two ports; Also, the ship's draught is considered to be constant because between two ports it does not unload or load cargo and fuel consumption affects the total mass of the ship in a small extent; Thruster, propeller, is adopted a fixed-step one, FPP, as a result of its coupling with an electric motor with an adjustable speed in wide limits.
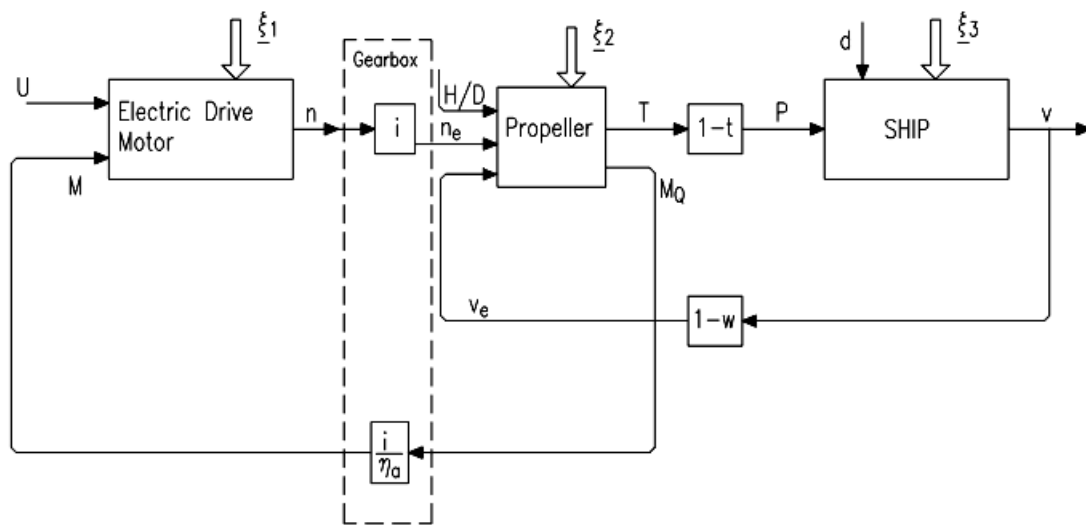


Fig. 4.1 – Structure of the Naval Electric Propulsion plant

The ship-engine – propeller system is described by the following two equations [CEA2]:

- The first equation that takes into account the dynamics of the ship's body is the form

$$m\frac{dv}{dt} = (1 - t) \cdot T(v, n_E) - R(v) \quad (4.1)$$

- The second equation describes the dynamic of the propelling

$$J\frac{d\omega}{dt} = M_M - M_Q(n_E, v) - M_F(n_E) \quad (4.2)$$

In the above equations, the following notations were made:

- m - Vessel Mass;

- v – The speed of the ship's rectilinear movement;

- T(v,n$_E$) – Thrust of the ship's thruster;

- t – The suction coefficient introduced as a result of only part of the thrust of the T-ship is found in the propulsion force, P, Fig. 4.1;

- R(v) – Hull resistance to rectilinear advance;

- J – Total inertion of the drive engine, propeller and shaft line;

- ω – Angular speed of the propelling in rad/sec;

- n$_E$ – The rotational speed of the propeller in rot/sec;

- $M_M$ – The active torque supplied by the engine;
- $M_Q$ – Strong propelling torque;
- $M_F$ – Resistant torque of system friction.

To solve the equations of the model it is necessary to knowledge the thrust characteristics of the T-ship and R-forward resistance, as well as the strong torque of the $M_Q$ thruster.

The propellers generate a thrust of the form:

$$T = k_T \cdot \rho \cdot D^4 \cdot n_E^2 \qquad (4.3)$$

Where $n_E$, propeller speed, in rev/s, is given by the relationship

$$n_E = \frac{n}{i} \qquad (4.4)$$

n being the engine speed, and i gearbox reduction coefficient.

D is the propeller diameter, $\rho$ sea water density, and

$$k_T = k_T(\lambda, H/D) \qquad (4.5)$$

function that is provided by the propulsion manufacturer, in graphic form, pending on the propeller step H/D and the parameter $\lambda$ the relative advance coefficient defined by

$$\lambda = \frac{v_E}{n_E \cdot D} (4.6)$$

The linear speed at the propeller level is lower than that of the vessel as a result of the siage phenomenon and is determined from

$$v_E = v \cdot (1 - w) \,(4.7)$$

where w is the siage coefficient.

The thruster generates the resistant torque to the drive engine shaft:

$$M = M_Q \frac{i}{\eta_o} \qquad (4.8)$$

where

$$M_Q = k_Q \cdot \rho \cdot D^5 \cdot n_e^2 \qquad (4.9)$$

Is the resistant torque generated by the propeller, and $\eta_o$ gearbox efficiency. Coefficient $k_Q$, just like $k_T$, is given by the propeller provider as a function of the form

$$k_Q = k_Q(\lambda, H/D) \qquad (4.10)$$

Being used in the same way.

The resistance to the ship's advance shall be determined

$$R = k_R \cdot v^a \qquad (4.11)$$

where $k_R$ and I take into account the draught of ship D and the condition of the hull. The two coefficients are provided, for a type of vessel, on the basis of the pool samples.

## 4.2. SHIP MODEL IN STEADY STATE REGIME

The hydrodynamic characteristics of the system, established by experimental or theoretical methods, are valid for stationary regimes being put in the form of relationships between the adimensional

coefficients $k_T$, $K_Q$, $\lambda$ and parameters of dynamic and Cinemics, T, Q and v. On the other hand the equation (4.1) becomes

$$(1-t)\cdot T(v,n_E) - R(v) = 0 \qquad (4.12)$$

The explicit feature of the hull, the equation (4.11), considering the resistance to the quadratic type, a=2, valid for most of the commercial vessel's deficiencies, can be put in a shape similar to the equation (4.3)

$$R = k_C \cdot \rho \cdot D^4 \cdot n_E^2 \qquad (4.13)$$

or in the form

$$k_C = \frac{R}{\rho \cdot D^4 \cdot n_E^2} = \frac{k_R \cdot v^2}{\rho \cdot D^4 \cdot n_E^2} \qquad (4.14)$$

In which by $k_C$ the hull thrust coefficient, like properties with $k_T$, was designated. Given the equation (4.12) and (4.3) and the siage effect, the coefficient $k_C$ is rewritten in the form of

$$R = k_C \cdot \rho \cdot D^4 \cdot n_E^2 \qquad (4.13)$$

or in the form

$$k_C = \frac{R}{\rho \cdot D^4 \cdot n_E^2} = \frac{k_R \cdot v^2}{\rho \cdot D^4 \cdot n_E^2} \qquad (4.14)$$

In which by $k_C$ the hull thrust coefficient, like properties with $k_T$, was designated. Given the equation (4.12) and (4.3) and the siage effect, the coefficient $k_C$ is rewritten in the form of the default feature of the Hull:

$$k_T^C = \frac{R}{(1-t)\cdot \rho \cdot D^4 \cdot n_E^2} = \frac{k_R}{D^2 \cdot \rho \cdot (1-w)\cdot (1-t)} \cdot \frac{v^2}{n_E^2 \cdot D^2} = c \cdot \lambda^2 \quad (4.15)$$

Where constant C has the expression

$$c = \frac{k_R}{D^2 \cdot \rho \cdot (1-w)^2 \cdot (1-t)} \qquad (4.16)$$

Obviously in steady state regime:

$$k_T^C = k_T \quad (4.17)$$

Where the thrusting coefficient of the propeller $k_T$ is supplied in graphical form as a function of relative advance $\lambda$ and H/D the propeller's step. At the intersection of the two characteristics, $k_t^C(\lambda)$ and $k_t(H/D, \lambda)$ the stationary operating point will be found.

The propeller efficiency can also be defined by

$$\eta_E = \frac{\lambda}{2\pi} \cdot \frac{k_T\left(\lambda, \frac{H}{D}\right)}{k_Q\left(\lambda, \frac{H}{D}\right)} \qquad (4.18)$$

which is also provided in graphical form.

## 4.3. SHIP MODEL IN DYNAMIC REGIME

Engine assembly Ship Model–Propeller–Hull is presented by equations (4.1) and (4.2). The major difficulty of integrating the model is generated by the essential unfairness of the default characteristics

$K_T(\lambda, H/d)$ and $K_Q(\lambda, H/d)$, provided on experimental basis in the form of diagrams or tables. To obtain explicit features, T, $M_Q$ and R, system resolution leads to Solutions V (t) and N (t), which give the time evolution of the kinematic parameters of the ship-propeller system. Considering the above conditions as well as the needs of initial ones for the simulation of steady state regimes the following strategy is proposed.

It approximates the polyomial characteristics $K_T(\lambda, H/d)$ and $K_Q(\lambda, h/d)$ supplied by the manufacturer in graphical form, [CAT1, CAT2]. Calculated at each step of integration, based on the current kinematic parameters of the system, the relative advance $\lambda$. On the basis of the calculated relative advance, the explicit characteristics T, $M_Q$ and R and a new kinematic is determined. The proposed method ensures accurately achieving the proposed steady state regime instead the dynamic part, accelerating from rest to the regime of marching or stopping the ship is not rigorously determined. Whereas in the paper only the steady state regime generated by the ship's march we appreciate that the proposed method is operative, real and useful.

## 4.4. SHIP SIMULATION

The SIMULINK model scheme of the ship considered is shown in Fig. 4.3. It comes from the analysis of the ship model, Fig. 4.1. by calculating the parameters according to the imposed propulsion data [CAT1, CAT2]:

- Shipl mass, m = 10,000 tonnes;
- March speed, v = 9m/sec;
- Propeller diameter, D=5.7m;
- Propeller type: FPP with H/D=1.32;
- Draught minimum, d=6.03m, $k_R$=1289.63:
- Coefficient of suction, t=0.2;
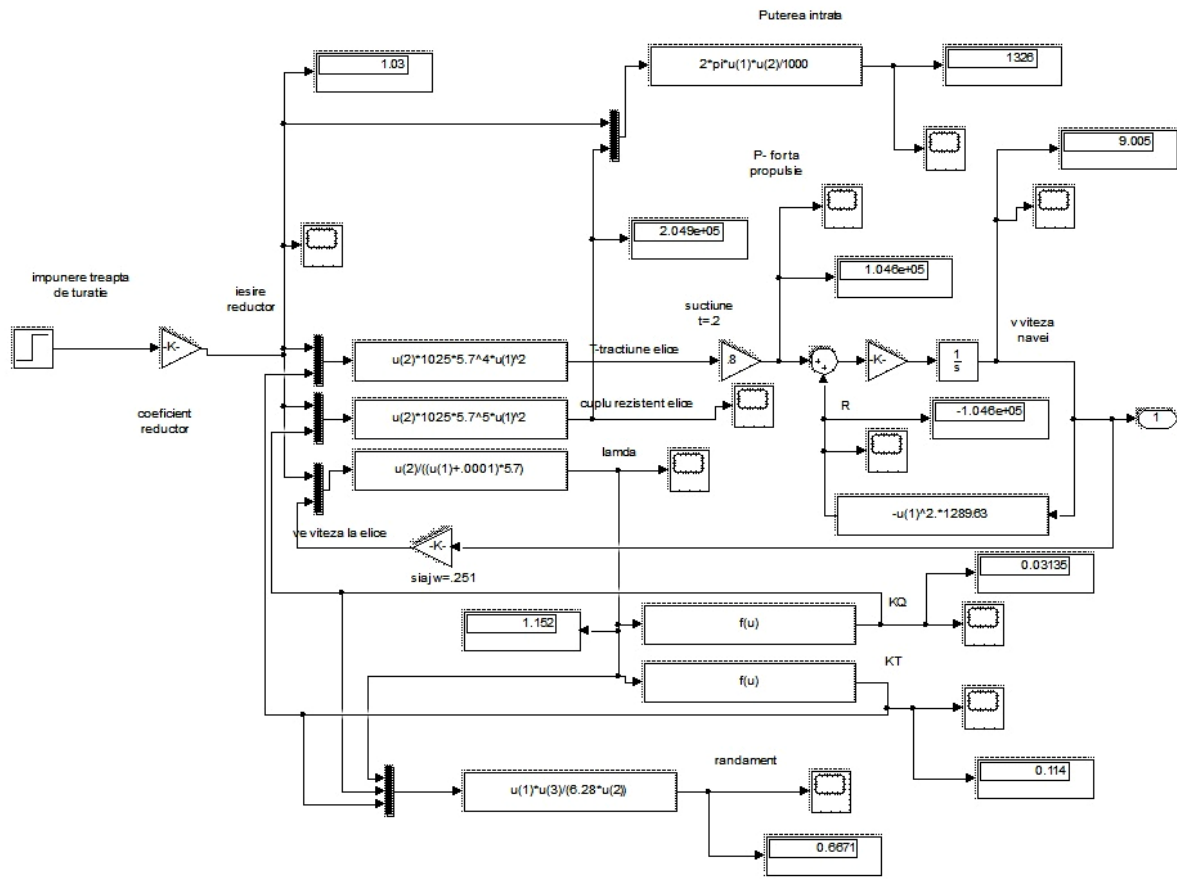- Siage coefficient, w=0.249;
- Gearbox transmission ratio, i=3.71.

Fig. 4.3 – SIMULINK Ship Model

It approximates polyomial, through a 5 grade polynome, the default characteristics $k_T(\lambda, H/d)$ and $k_Q(\lambda, H/d)$ resulting in:

$$k_T = -2.4858 \cdot \lambda^5 + 8.6446 \cdot \lambda^4 - 11.6176 \cdot \lambda^3 + 7.4511 \cdot \lambda^2 - 2.7144 \cdot \lambda + 0.9326$$

$$k_Q = 0.3349 \cdot \lambda^5 - 1.2136 \cdot \lambda^4 + 1.6522 \cdot \lambda^3 - 1.0618 \cdot \lambda^2 - 0.2388 \cdot \lambda + 0.0928 \tag{4.19}$$

Which ensures an accuracy of calculation around 0.1%.

Calculate the explicit feature of the hull resistance in advance by

$$c = \frac{k_R}{\rho \cdot (1-w) \cdot (1-t) \cdot D^2} = \frac{1289.63}{1025 \cdot 0.749^2 \cdot 0.8 \cdot 5.7^2} = 0.08628 \tag{4.20}$$

and the equation for determining the relatively advance λ is formed:

$$0,08628 \cdot \lambda^2 = k_T(\lambda, H/D) \tag{4.21}$$

From solving which is obtained

$$\lambda = 1,517 \tag{4.22}$$

Calculate the required propeller speed

$$n_E = \frac{(1-w) \cdot v}{\lambda \cdot D} \tag{4.23}$$

and to the driving engine level.

$$n = 2 \cdot \pi \cdot n_E = 24 \frac{rot}{s} \qquad (4.24)$$

The calculated propeller efficiency in Fig. 1.2 has the value

$$\eta = 0{,}67 \qquad (4.25)$$

The validation of the designed model was performed by simulation in MATLAB SIMULINK in accordance with Fig. 4.3 without taking into account the dynamics of the motor-propeller system, dynamic which is much faster than the propeller-hull.
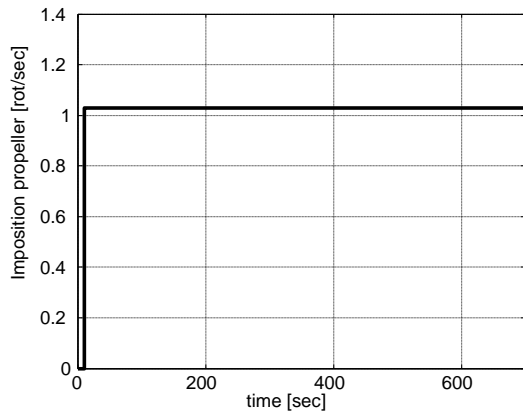


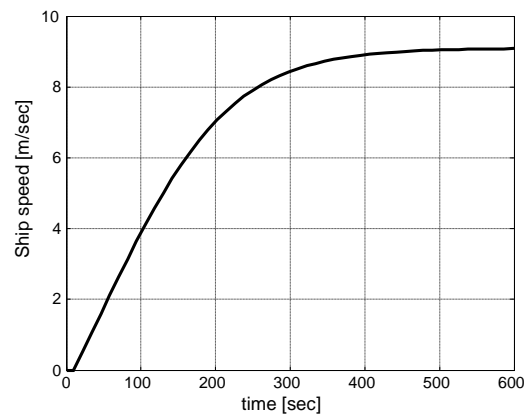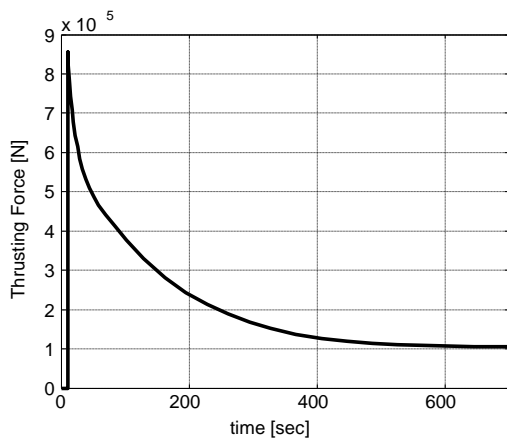Fig. 4.4 – Imposing the propeller speed



Fig. 4.5 – Ship speed

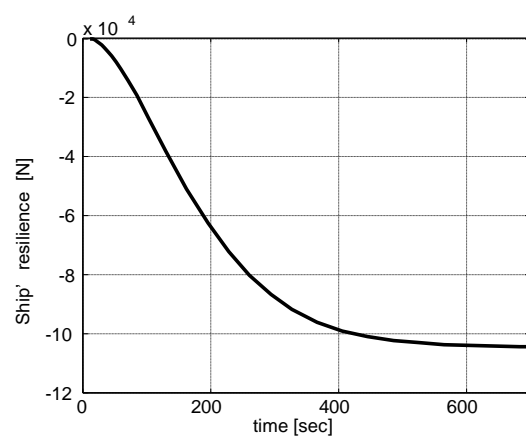

Fig. 4.6 – Thrusting force



Fig. 4.7 – Ship's resilience

The model was excitated by a nominal speed applied to the propeller, 1.03 rpm as per Fig. 4.4 and infinite power. In Fig. 4.5, 4.6 and 4.7 the ship's speed, thrusting force and ship's resilience are presented. The steady-state regime is presented in table 4.1.

Table 4.1

|  | $V_N$ | $n_E$ | $n_M$ | $M_Q$ | $P_Q$ | λ | η |
|---|---|---|---|---|---|---|---|
|  | m/s | rot/s | rot/s | kNm | kW |  |  |
| H/D 1.320 | 9,0 | 1,03 | 24 | 205,8 | 1231 | 1,151 | 0,67 |

From the graph analysis and the steady state regime presented in Table 4.1 the results the following:

- The steady state regime obtained by simulation is identical to the calculated one;
- Propeller efficiency η = 0,67 is in the maximum efficiency area [CAT1, CAT2];
- The relative advance λ is consistent with the calculated one even if it has different values during the dynamic ship acceleration regime;
- Slow dynamics is caused by the high mass of the ship and the evolution of the ship's resilience;
- At controllable pitch propellers, CPP's, the calculation procedure is the same taking into account the corresponding diagrams from [CAT1, CAT2].

## 4.5. FPP OR CPP?

The propulsion of ships requires, in principle, two basic requirements: ensuring the prescribed speed of the ship's marching and minimizing fuel consumption.

When the thruster is fixed-pitch, the FPP can only ensure the first requirement by modifying the propeller speed. If the propeller is adjustable, the CPP, the order has two degrees of freedom and both of these requirements can be imposed [FRA1].

Any approach in the area of the criteria for assessing the profitability of the ships requires at first instance the analysis of the possibilities to reduce fuel consumption per tonne of freight transported per mile traveled.

The use of the adjustable pitch propeller (CPP) was mainly imposed with the use of semirapide propulsion engines to which it was chosen to reverse the marching direction by installing the CPP.

This type of propeller creates a degree of freedom in optimization because the speed parameter can be adjusted as well as the step H/D ratio, unlike the fixed-pitch propeller where the only adjustable element is the engine speed.

These two adjustable factors, the step ratio and the cough must be corroborated against each other appropriately to ensure full use and maximum efficiency. It is important to ensure that any adjustment made to one of the two units (engine and propeller) must not force an unfavourable or inadmissible state of operation to the other.

In connection with the ship, the CPP may give an effective (or net more efficient) response to the modification of the external conditions occurring during operation, i.e. the modification of the resistance to the projected conditions.

In the case of EPR, the date marching speed can be achieved at different values of the speed of the propeller and the step ratio, which is why you can always choose the most economical movement regime, so the most convenient combination between step and speed.

Another advantage that must be mentioned is also linked to the minimum speed of the ship, which is determined by the minimum steady engine speed. For diesel engines, this limit is high, with a limit of 35-40% of the nominal one. The CPP installation allows you to obtain any speed value from zero to maximum even at nominal speed. Reducing the speed of the ship is achieved by decreasing the step, the speed of the porcelain shaft maintaining constant.

In order to make the two variants more clearly evident, CPP and FPP when using the electrical actuation, 3 simulations were performed for the above model under the following conditions:

- March 9 m/sec and EPF with pitch ratio H/D 1320 and propeller speed 1.03 rpm, corresponding to 24 rpm/sec at the engine shaft level;

- Keeping the engine speed constant at 24 rpm/sec simulated the model for CPP with step H/D reports 1.020, 0.856 and 0.725.

    The obtained data were recorded in Table 4.2.

Table 4.2.

| | $V_N$ m/sec | $n_E$ rot/sec | $n_M$ rot/sec | $M_Q$ kNm | $P_Q$ kW | $\lambda$ | $\eta$ | $\lambda_M$ |
|---|---|---|---|---|---|---|---|---|
| **H/D 1.320** | 9,0 | 1,03 | 24 | 205,8 | 1231 | 1,151 | 0,67 | 0,67 |
| **H/D 1.020** | 7,198 | 1,03 | 24 | 117,2 | 758,2 | 0,92 | 0,58 | 0,65 |
| **H/D 0.856** | 6,22 | 1,03 | 24 | 84,92 | 549,4 | 0,796 | 0,53 | 0,58 |
| **H/D 0.725** | 5,206 | 1.03 | 24 | 72,86 | 471,3 | 0,666 | 0,516 | 0,55 |

- As we expected, with the decrease of the step report, the ship's speed decreases although the propeller rotates steadily with 1.03 rpm. The relative advance decreases and the propeller efficiency is lower than the maximum, $\lambda_M$, supplied in [CAT1, CAT2];

**Table 4.3.**

| | $V_N$ m/sec | $n_E$ rot/sec | $n_M$ rot/sec | $M_Q$ kNm | $P_Q$ kW | $\lambda$ | $\eta$ |
|---|---|---|---|---|---|---|---|
| **H/D 1.320** | 9,0 | 1,03 | 24 | 205,8 | 1231 | 1,151 | 0,67 |
| **H/D 1.320** | 7,198 | 0,821 | 19,146 | 130,4 | 673,1 | 1,151 | 0.667 |
| **H/D 1.320** | 6,22 | 0,719 | 16,54 | 97,34 | 434,0 | 1,151 | 0,667 |
| **H/D 1.320** | 5,206 | 0,594 | 13,85 | 68,25 | 254,8 | 1,151 | 0,667 |

Variable forward speeds can be performed with FPP by modifying the speed of the electric motor, as per Table 4.3. There are several findings to be concluded:

- The prescribed speeds shall be achieved at a relatively steady-down advance, calculated for FPP with step H/D ratio 1.320;

- The propeller efficiency remains constant at the maximum value;

- The mechanical power required at the thruster shaft, $P_Q$, is less sensitive to FPP versus CPP, from 88.78% for H/D 1.020 to 54.06% for H/D 0.725.

    It follows that in the case of electric propulsion it is more favourable to use the FPP fixed-pitch propeller which operates at maximum efficiency. The electric motor must also be ordered to operate with minimal loss.

# CONVENTIONAL AUTOMATION OF NAVAL PROPULSION SYSTEMS WITH DC MACHINES

## 5.1. MODEL OF THE ACTUATION SYSTEM

The parameters of the actuation system taken into account are:

| | |
|---|---|
| Nominal power | $P_N$=6500 [kW] |
| Rated speed | $n_N$=375/750[rpm] |
| Rotoric voltage | $U_{AN}$=1000[V] |
| Stator voltage | $U_{EN}$=310[V] |
| Rotor nominal current | $I_{AN}$=6915A |
| Rotor maximum current | $I_{AM}$=2$I_{AN}$=13830A |

| Stator nominal current | $I_{EN}$=30A |
| Nominal torque | $M_N$=166 [kNm] |
| Maximum torque | $M_M$=2$M_N$=332 [kNm] |
| Rotoric resistance | $R_A$=4.3 [mΩ] |
| Stator resistance | $R_E$=10,45[Ω] |
| Rotor inductivity | $L_A$=0,146[mH] |
| Stator inductivity | $L_E$=5,84 [H] |
| Total inertion moment | J=900[kgm$^2$] |
| Electric motor constant | k=0,808 |
| Viscous friction coefficient | $F_v$=135,27 |

Model equations are given by equation system [PĂD 11]

$$\frac{di_A(t)}{dt} = \frac{u_A(t)}{L_A} - \frac{R_A}{L_A} \cdot i_A(t) - \frac{1}{L_A} \cdot \frac{1}{L_A} \cdot ki_E(t) \cdot \omega(t)$$

$$\frac{di_E(t)}{dt} = \frac{u_E(t)}{L_E} - \frac{R_E}{L_e} \cdot i_E(t) \text{ (5.1)}$$

$$\frac{d\omega(t)}{dt} = \frac{1}{J} \cdot ki_A(t) \cdot i_E(t) - \frac{F_V}{J} \cdot \omega(t) - \frac{1}{J} \cdot m_R(t)$$

where:

$m_m = ki_E \cdot i_A$ - torque developed by the machine;

$e_{mf} = ki_E\omega$ – Electromotor voltage;

$u_A, u_E$ – Rotor voltage, stator voltage;

$i_A, i_E$ – Rotor Current, stator current;

$R_A, R_E, L_A, L_E$ – Resistance and inductivity of the rotor, respectively of the stator;

$k$ – Electric motor constant;

$F_v$ – Viscous friction coefficient;

$J$ – Inertion moment;

$m_R$ – Rezistant torque.

## 5.2. CONVENTIONAL AUTOMATIC CONTROL

Conventional automatic control is achieved by the principle of electromotive voltage adjustment being usable for both constant and variable flow adjustment [PAD 11]. The block control diagram is presented in Fig. 5.2. The rotor circuit is controlled by two regulators, the $R_{IA}$ for the rotors and Rω current for angular speed, cascade connected in the order of time constants, the faster current loop, being the inner one [01].
   The design of the regulators was made using the well-known criteria of the module and symmetry.
If the speed adjustment is also done by deexcitation, $k_{iE}$ is variable in size, depending on the excitation current by the machine's magnetization feature. This unethality is neglected as a result of low-limit unexiting, 1/2.... 1/3, somewhat corresponding to the linear portion of the magnetization feature.
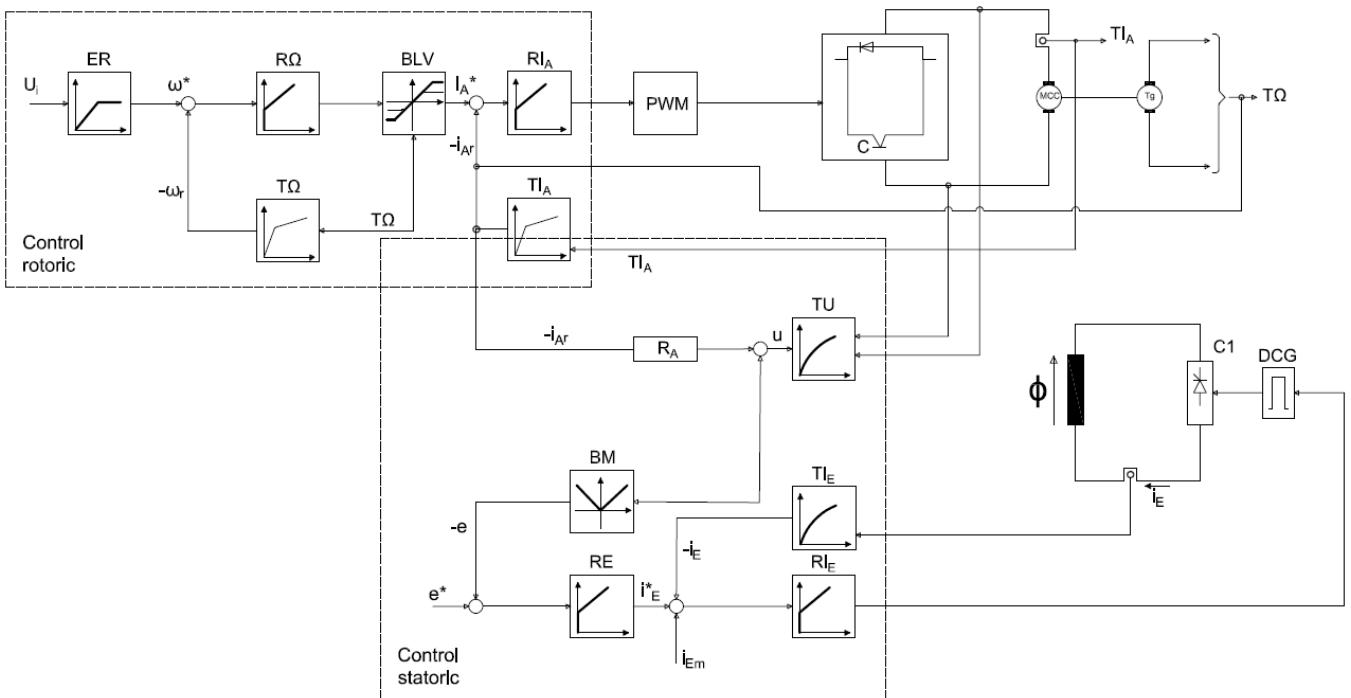
Fig. 5.2 – Automatic control of an actuation system with DC motor at constant and variable flow

The size of $k_{iE}$ affects the parameters of the speed regulator and the consequence of dynamic behavior of the machine. Solutions to overcome the problem are as follows: adaptive regulator and a compromise between dynamic system performance and regulator parameters.

The second problem is generated by the necessity, in some machines, of limiting the rotor current for higher speeds for switching reasons. Usually the limitation is variable, depending on the size of the speed, and is performed in Fig. 5.2. Through the BLV block, variable limitation block. The calculation of the excitation current regulator is identical to that of the rotoric current, while the electromotive voltage regulator is calculated by experimental methods. The electromotive voltage adjustment loop is considering its constant retention at nominal value,

$$E_N = U_{AN} - R_A \cdot I_{AN} = k \cdot \Omega \cdot I_E = cst \quad (5.12)$$

When, as a result of deexiting, the speed rises to values above those on the natural mechanical characteristic. In Fig. 5.5 and 5.6. Two acceleration processes from resting up to the nominal/maximum speed for the nominal step applied to t=4 seconds are presented, the replies obtained fully confirm the model of the D actuation systemopted.
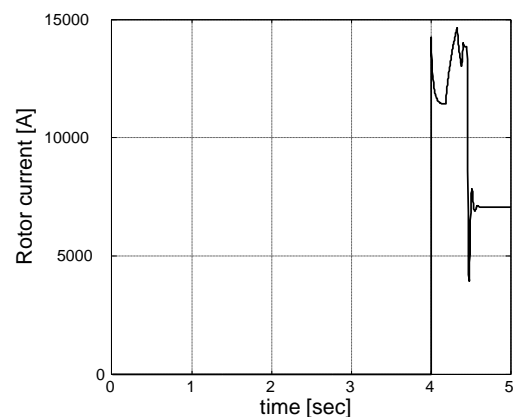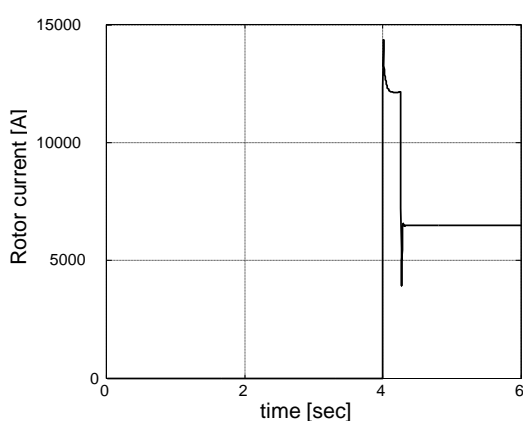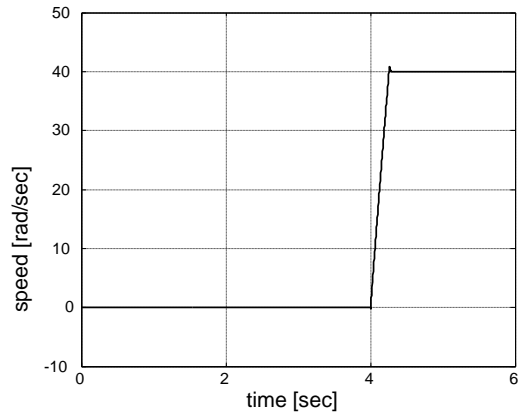
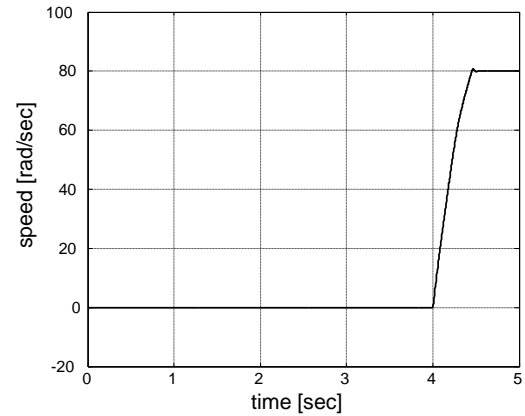Fig. 5.5.  Steady flow acceleration                Fig.5. 6. Variable Flow acceleration

## 5.3.  AUTOMATIC CONTROL FOR SHIP PROPULSION

The adjustment system presented above did not take into account the characteristics of the load so the evolution of the durable torque created by the propeller. It is known that for the adopted model and use of the criteria for granting the above regulators, the total rejection of the essential disruptive size of the system, the durable static torque, is ensured. To highlight this, the global simulation scheme was drawn up., by coupling the model of the actuator with the vessel pattern designed in Chapter 4. It requires a single modification consisting in linking the required speed to propeller, propellant, with that supplied by the engine. The nominal engine speed shall be adopted,

$$n_M = 375 \frac{rot}{min} = 40 \frac{rad}{sec} \quad (5.17)$$

To achieve the speed of marching. The correlation is carried out by the mechanical reducer that will have to have the transmission ratio

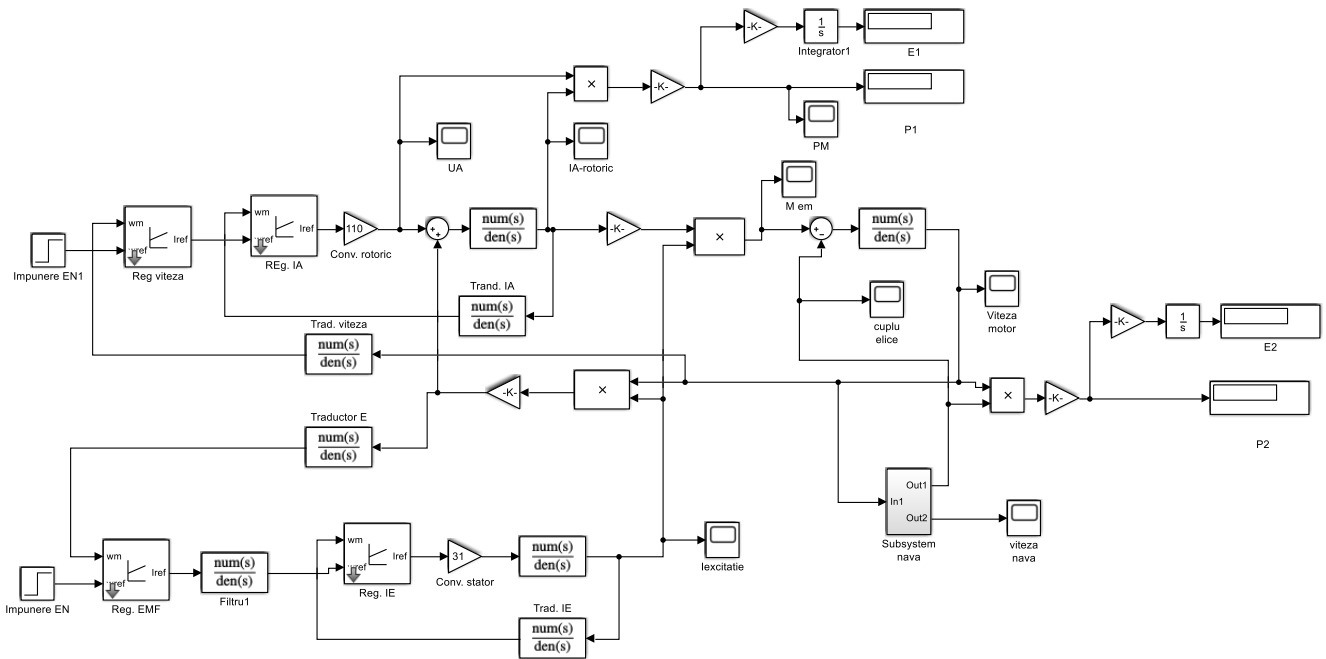$$i = \frac{n_M}{n_E} = 6,18 \ (5.18)$$

Fig. 5.8 – Simulink Ship Propulsion Model

The simulation was carried out under the same conditions as the vessel model, Chapter 4, was validated. Thus for an FPP propeller with H/D = 1.320 and the ship speed imposition v=9 m/sec were obtained the replies from Fig. 5.12 and 5.14, identical to those made for the ship model, excited with a nominal angular speed signal.
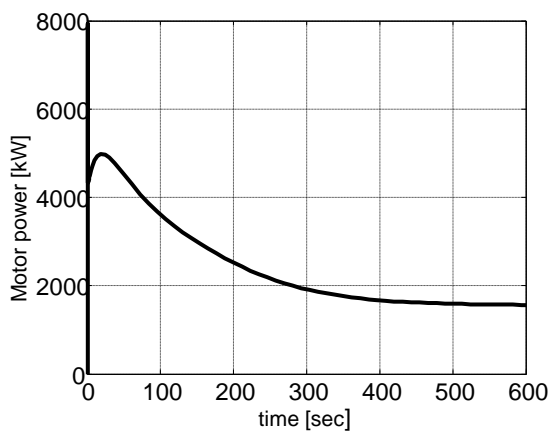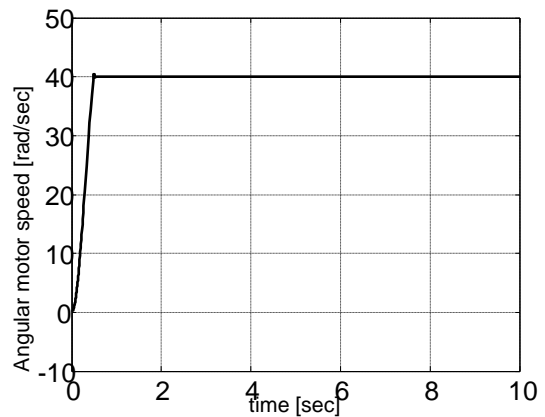


Fig. 5.14 – Motor power



Fig. 5.12   Angular motor speed

Essentially the actuation system comprises two dynamics, a fast one – the electric motor, the reducer and the propeller and the other slow one – propeller and ship. The first dynamic is not affected in any way by coupling the ship model, the rotor current and the engine speed, Fig. 5.12. The response time being those presented for conventional automation in Fig. 5.5. and 5.6. The propeller dynamics – ship is a very slow one, reaching the marching speed as per Fig. 5.9 is achieved after about 600 seconds,

which is not too favorable. This behavior is generated by the way the transfer of power from the propeller to the ship, highlighted by the variation of the propeller-resistant torque. It also finds a poor use of the electric motor, starting from 8000kW, at the earliest moments of the start as a result of the first dynamic and gradually decreasing to about 1575 kW at the entrance to the steady-state mode of marching. In order to improve the second dynamic, the control diagram in Fig. 5.15 is proposed.
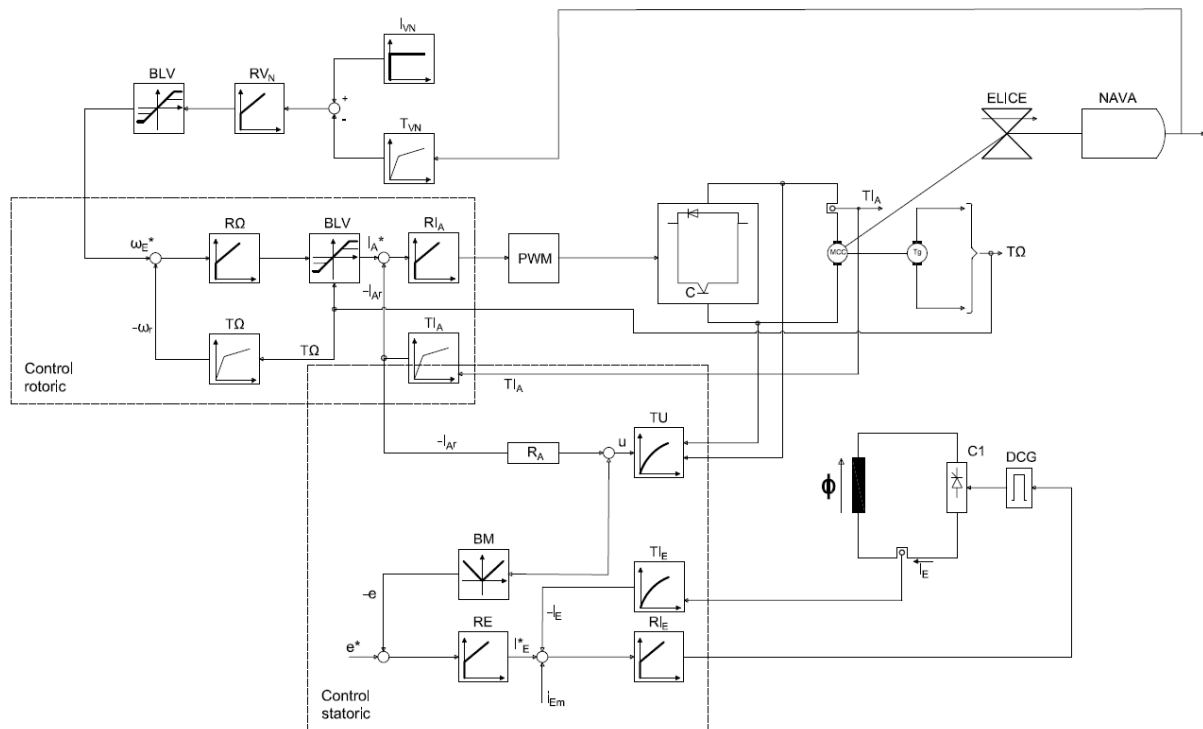


Fig. 5.15 – Automatic Ship speed control

The idea of the proposed control leaves the following observations characteristic of conventional automation:

- The speed of the ship is indirectly controlled by adjusting the speed of the propelling;
- The transfer of power from the propeller to the ship is made naturally, without being controlled;
- The duration of the ship's starting process from resting to the speed of marching, also uncontrollable, far too high in relation to the properties of the electrical actuation.
  To improve the performance of the dynamic propulsion regime, in the control diagram in Fig. 5.15. Insert an external adjustment loop of the ship's speed, V. This is possible as a result of the much slower dynamic of the ship in relation to the dynamics of the electric motor-propeller.

The following conclusions are drawn from the analysis of the simulation results:

- The acceleration time of the ship up to the marching speed decreased considerably, with a value of about 140 seconds, Fig. 5.17;
- Variations of the propelling torque, Fig. 5.18 as well as engine power Fig. 5.21, and Rotor Current, Fig. 5.22 are flattened pretty much during the starting period being beneficial for the operation of the engine;

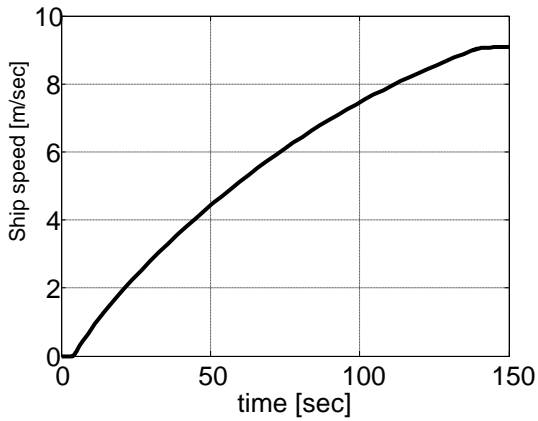- The propeller speed shall be kept steady at the required value, Fig. 5.20.
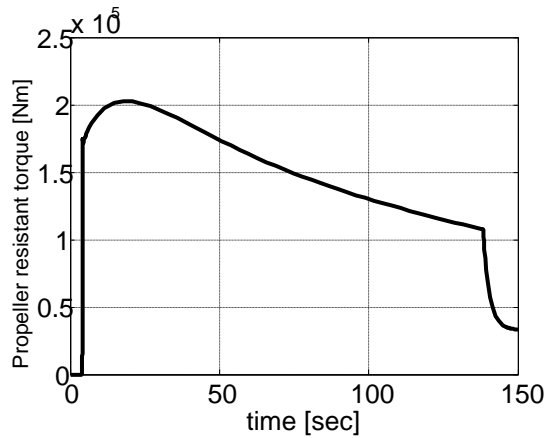
Fig. 5.17 – Ship speed

Fig. 5.18 – Propeller resistant torque

Fig. 5.21 – Rotor current

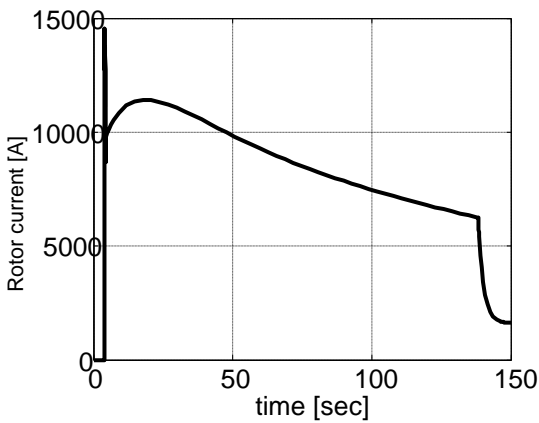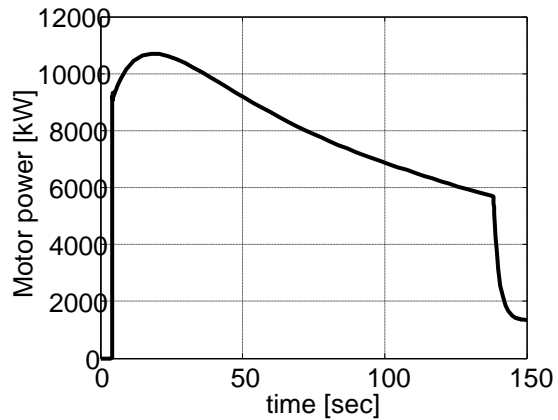Fig. 5.22 – Motor power

- The propeller speed is higher than the nominal, marching one, the propeller must be appropriately dimensioned, i.e. allow the speed of 52.8 radians/second;
- The actual output of the above speed, higher than the nominal one, can obviously only be achieved by deexcitation, the state current being shown in Fig. 5.23.
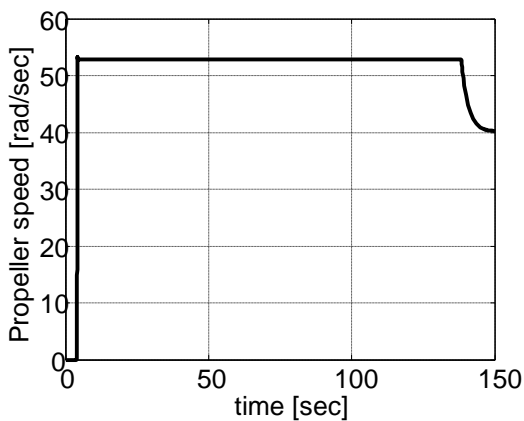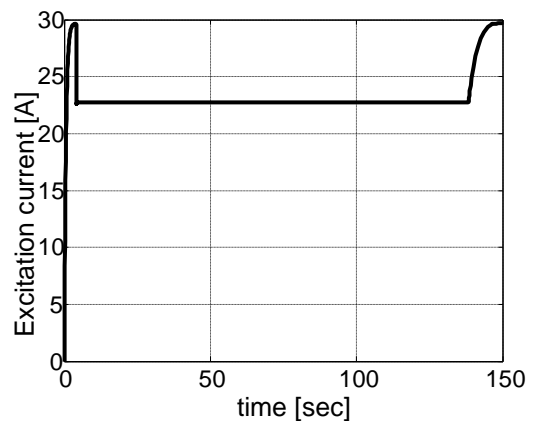
Fig. 5.20 –Propeller speed

Fig. 5.23 – Excitation current

Overall the proposed solution is favourable from almost all points of view. The only vulnerable point is generated by over-speed thruster by about 50%, which probably has some consequences for the design of the propeller.

# 6. CONVENTIONAL AUTOMATION OF THE PROPULSION SYSTEM WITH THREE PHASE INDUCTION MACHINES

## 6.1. MATHEMATICAL MODELS OF THE DRIVING SYSTEM

Mathematical modelling was performed, for the three-phase induction machine with rotor in short circuit.

By adopting the model in voltages with orientation after the rotoric magnetic field, characterized by the set of equations [LEO 85],[MUN 11]:

$$\frac{u_{d1}}{R_1} = i_{d1} - \omega_1 \cdot \sigma \cdot T_1 \cdot i_{q1} + \sigma \cdot T_1 \frac{di_{d1}}{dt} + (1 - \sigma) \cdot T_1 \frac{di_{m2}}{dt} \quad (6.1)$$

$$\frac{u_{q1}}{R1} = i_{q1} + \omega_1 \cdot \sigma \cdot T_1 \cdot i_{d1} + \sigma \cdot T_1 \cdot i_{d1} + \sigma \cdot T_1 \frac{di_{q1}}{dt} + \omega_1 \cdot (1 - \sigma) \cdot i_{m2} \quad (6.2)$$

$$T_2 \cdot \frac{di_{m2}}{dt} + i_{m2} = i_{d1} \quad (6.3)$$

$$\omega_1 = p \cdot \omega + \frac{p \cdot i_{q1}}{T_2 \cdot i_{m2}} \quad (6.4)$$

$$J \cdot \frac{d\omega}{dt} = m - F_v \cdot \omega - m_r \quad (6.5)$$

$$\frac{d\theta}{dt} = \omega_1 \quad (6.6)$$

- $u_{d1}$, $u_{q1}$, $i_{d1}$, $i_{q1}$ are the symmetrical d/q components of the static voltage and currents;
- $i_{m2}$ rotor magnetization current;
- $R_1$ si $R_2$ resistances on a phase of the stator and rotoric winding;
- $T_1 = \frac{L_1}{R_1}$ și $T_2 = \frac{L_2}{R_2}$ are the time constants of the statoric and rotoric winding-up;
- $m = \frac{3}{2} \cdot \frac{p}{1 + \sigma_2} \cdot L_m \cdot i_{m2} \cdot i_{q1}$ electromagnetic torque of the machine;
- $\omega_1$ Synchronism speed;
- $\omega$ Angular speed at the machine shaft;
- $m_r$ Resistant static torque;
- $F_v$ Viscous friction coefficient;
- $\Theta$ Orientation angle by rotors magnetic field;
- $p$ Number of pairs of poles;
- $\sigma = 1 - \frac{1}{(1 + \sigma_1) \cdot (1 + \sigma_2)}$ Total magnetic coupling coefficient;
- $L_1$, $L_2$, $L_m$ Inductivities of Stator and rotor and mutual coupling, respectively;

- $\sigma_1$, $\sigma_2$ magnetic coupling coefficients of stator and rotoric winding.

Analyzing the two proposed structures results in a nonlinear process generated by:

- Products between the status sizes;
- Variable parameters depending on the temperature of the machine, mainly the change in the value of the rotoric resistance and magnetic saturation, especially in the case of operation at varying power frequency.

For electric propulsion with three-phase induction machine, the engine with parameters has been adopted:

- Nominal power, 6300 kW;
- Rated voltage, 3x6000/3464 V, 50Hz;
- Rated current, 703 A;
- Nominal torque, 40400 Nm;
- Critical torque, 80800 Nm;
- Rated speed, 1491 rev/min, 156.1 rad/sec;
- Number of pairs of poles, p = 2;
- The resistance of the stator winding, $R_1$= 72.5 m$\omega$;
- Inductivity of stator Winding, $L_1$= 0.0667 No;
- Resistance of the rotoric winding, $R_2$= 25.6 m$\omega$;
- Inductivity of the Rotoric winding, $L_2$= 0, 0667h;
- Magnetization inductivity, $L_m$= 0.0651 H;
- Coefficient of viscous friction, $K_V$= 1.53;
- Total Moment of inertia, engine, reducer and propeller, J = 200 Kgm2;
- Total coefficient of magnetic magnetic coupling $\sigma$ = 0,0582;
- Torque coefficient $k_m$= 0.189.

Power sources with potential for use in naval propulsion are PWM inverters and cycloconverters. They were modeled through linear and non-inertial amplifiers, with kd amplification factor=1200, which is very close to reality.

### 6.3. Conventional automation

Frequently adjustable actuation systems with three-phase induction machines and rotor in short circuit are used in two operating regimens:

1. At angle speeds less than or equal to those on the nominal mechanical feature, the so-called steady U/f regime, which preserves the critical, maximum electromagnetic torque of the machine, being advantageous to use for low speeds and large resistant static couples

2. At speeds higher than those on the natural mechanical feature, with considerable shrinking of the critical torque, also called a flow reduction, conducive to high speeds and small couples. The regime is carried out keeping the constant supply voltage, usually at the nominal value, and the frequency higher than the nominal.

The conventional automatic control is structured after the two channels, d and q, and after the specifics of the quick processes, that is, a cascading adjustment with type P and PI regulators, which

are placed in order of the size of time constants of the controlled parameters. The determination of the type of regulator and the calculation of the parameters of the agreement are two difficult problems due to the fact that the equations (6.8) of the system, used for calculating symmetrical components of the static current, are nonlinear. Overcoming this inconvenience is achieved by rewriting the equations in question in another form [LEO 85].
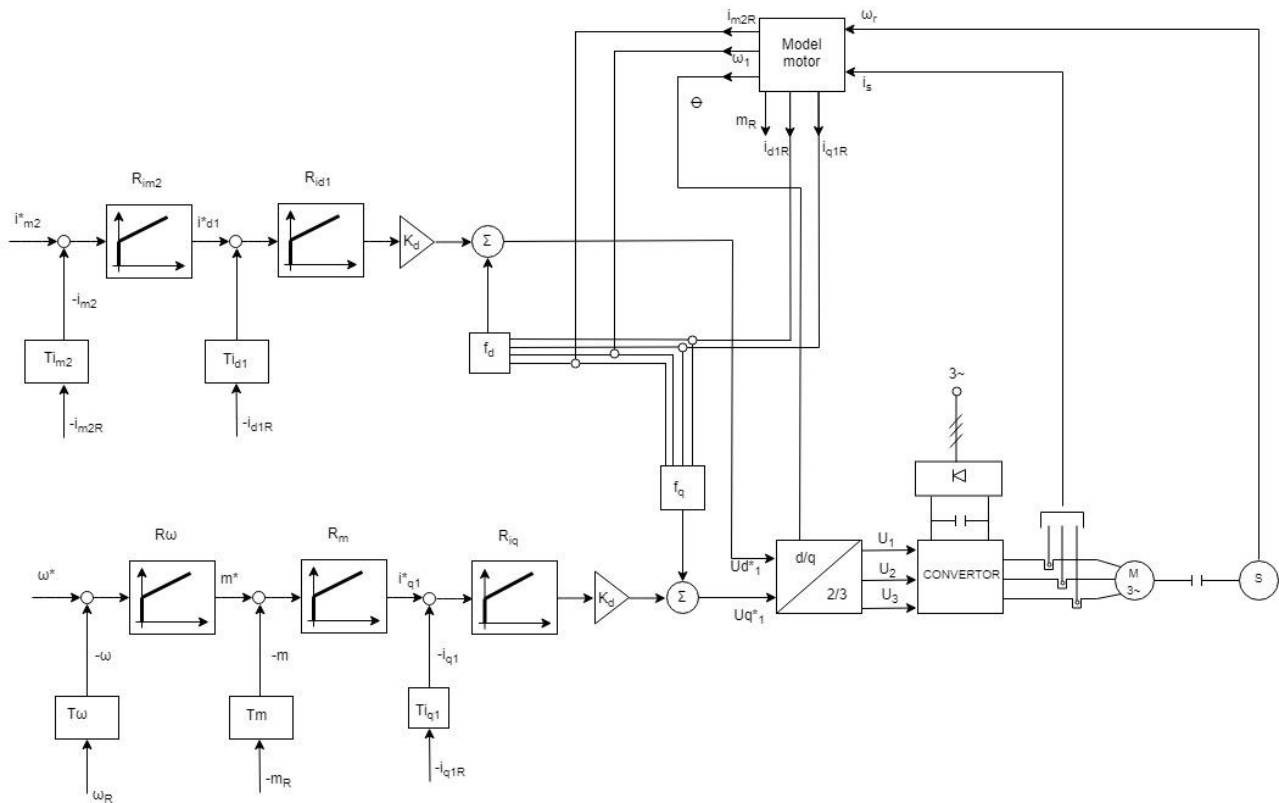


Fig. 6.3 – Constant flow control block diagram

With regard to variable flow adjustment, the control scheme leaves from the one in Fig. 6.3, supplemented by the Rdo voltage regulator, fig. 6.4.  For operation at

$$\omega < \omega_N \quad (6.18)$$

where $\omega$ $and$ $\omega_N$ are the actual and nominal speed, the imposition of the rotors magnetization current is carried out in the same way as in the previous case, being applied to the $R_{IM2}$ regulator via switch C to position 1.. The control scheme works the same as in the constant flow case. For higher than nominal speeds, the rotors magnetization current shall be carried out by the Ruo voltage regulator and shall be applied further, by switch C, switched to position 2, regulator $R_{IM2}$.  The purpose of this adjustment is to keep the supply voltage steady, in accordance with the principle of variable flow operation. For this purpose, the reference voltage must be $U_0^\bullet$ , corresponding to the nominal voltage, and compares to the actual compuable voltage

$$U_R = \sqrt{\frac{V_d^2 + V_q^2}{2}} \quad (6.19)$$

$V_d$ and $V_q$ Can be calculated in the system model, Buo block, or assimilated with the resulting impunations $V_{d1}^*, V_{q1}^*$ ,



Fig.6.4. Variable flow control block diagram.

## 6.2. VALIDATION BY NUMERICAL SIMULATION OF CONVENTIONAL AUTOMATION

The validation of the two control schemes proposed above by numerical simulation in the MATLAB-SIMULINK environment takes into account the following objectives:

1.  Obtaining favourable dynamics for the parameters adjusted, without oscillations and with admissible over-adjustments;
2.  Carrying out with a minimum or null error of the quantities imposed, in the specific case, of the angular speed of the engine;
3.  Retention within permissible limits of electrical and mechanical sizes, voltages, currents, electromagnetic torque and angular speed;
4.  Making the best possible dynamics, starting, stopping, and changing the low speed.

The controllers provided are of the PI type, structure and parameters being determined by the Ziegler-Nichols method [CEA 01]. The rotors magnetization current control channel has different parameters for the two situations, U/f = constant and variable flow, due to the different structure of the controlled channel.

### 6.3.1. VALIDATION BY NUMERICAL SIMULATION FOR THE CONSTANT U/F CASE

A 5-second simulation programme divided into: 0 – 1 S, magnetization of the machine, has been established for numerical validation of the model and the automatic Cotrol. 1 – 3 S, starting up to synchronism speed by 25% of the durable torque; 3 – 5 s operation at torque and nominal speed. Analyzing the waveforms provided by the simulation, Fig. 6.6. ...... Fig. 6.12., the following conclusions result:

• All electrical and mechanical sizes have natural, physically achievable developments, without oscillations and with admissible over-adjustments. These things validate on the one hand the accuracy of the mathematical model used, and on the other hand the proper configuration and granting of the control system regulators.

• Angular velocity, Fig. 6.8., is performed with virtually null error. The growth of the static torque resistant to the nominal value leads to the occurrence of a stationary error of about a Radian/sec, 0.76%, which means that the control system ensures the rejection of the essential disturbance effect of the process, the durable static torque. The speed overage is insignificant from less than 1%, falling within admissible limits. The response time, for the first touch, is 0.7 seconds, characteristic of actuations with three-phase rotor induction machines in short circuit

• The Rotoric magnetization Current, Fig. 6.7., also has a very good dynamic, reaching the stationary value taking place in about 0.5 seconds, due to the fact that only the magnetization process takes place in this time frame.

Concluzie sistemul de control structurat răspunde tuturor cerințelor şi poate fi utilizat pentru dezvoltări ulterioare.
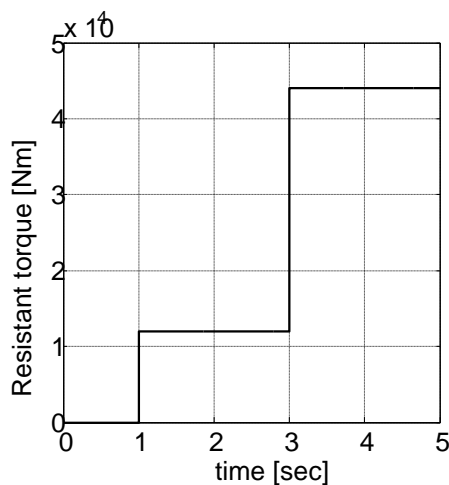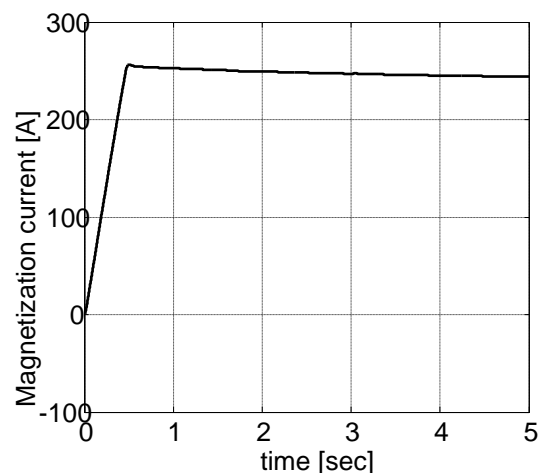
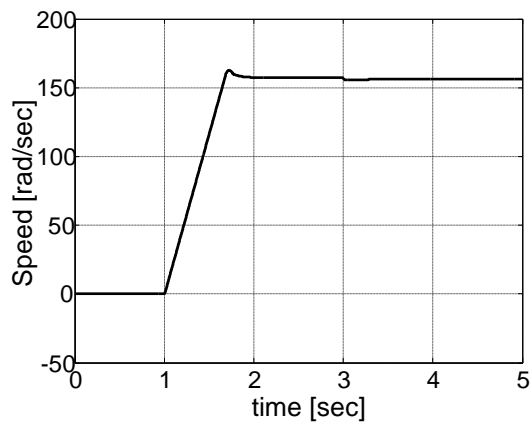Fig.6.6. Rezistant torque.

Fig. 6.7. Magnetization current.
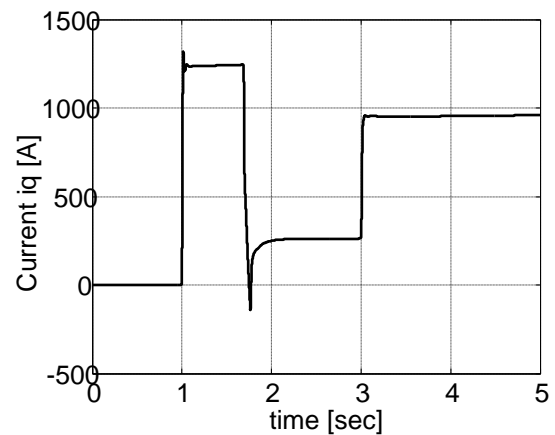
Fig.6.8 Angular speed.



Fig. 6.12. Current $i_q$.

### 6.3.2. VALIDATION BY NUMERICAL SIMULATION FOR THE U-CONSTANT AND F VARIABLE

A simulation program similar to the above 6-second duration consisting of:

• A first 2-second interval for machine magnetization;

• Second interval, between 2 seconds and 3.5 seconds for acceleration from sleep to synchronism speed with a 25% resistant torque;

• The third interval, between 3.5 and 6 seconds, to accelerate to double the speed of synchronism and stationary operation at this speed. At the time of 5s, the durable static torque in the form of a step is changed to 50%.

Analyzing the waveforms provided by the simulation, Fig. 6.15. ...... Fig. 6.21., the following conclusions are resulting:

• All electrical and mechanical sizes have natural physically achievable developments without oscillations and with admissible over-adjustments. In fact, the same adjustment, for accelerating from resting to angular speed of synchronism, angular velocity, Fig. 6.16., has the same performance as in the constant U/f case. The imposition for doubling the speed, the third interval, leads to a response similar to that of the previous case, that is, with virtually nil stationary error, low response time and linear speed variation. The increase of the static torque resistant to 20,000 Nm leads to the occurrence of a stationary error of the same order of magnitude as in the constant U/f case, which means that the control system also ensures the rejection of the effect of the essential disturbance of the process, the durable static torque.

• As regards the rotoric magnetization current, Fig. 6.17., the variation is completely different from the constant U/f case. The magnetization current regulator has in this case two functions: Premagnetization of the machine, identical to the constant U/f case; Decrease flow for variable f case.
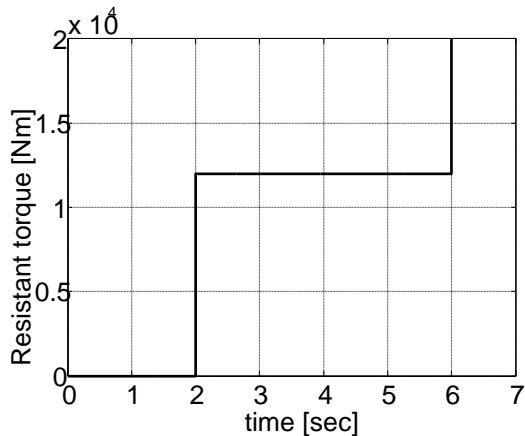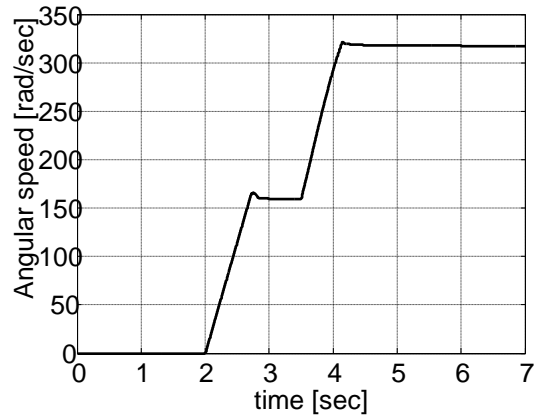
Fig. 6.15 – Resistant torque
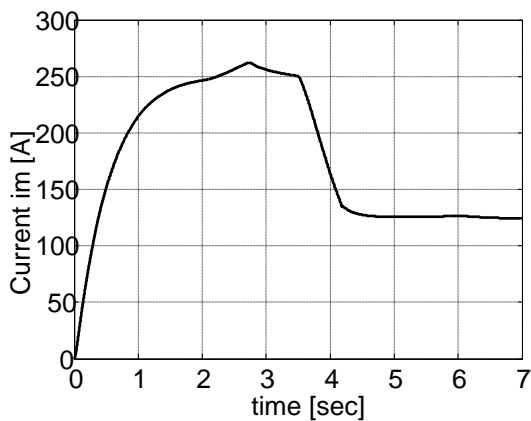


Fig. 6.16 – Angular speed
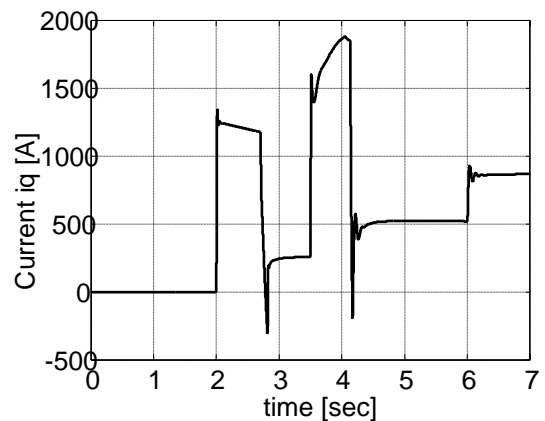


Fig. 6.17 – Magnetization current $i_m$



Fig. 6.19 – Current $i_q$.

The electric propulsion of the ship with the three-phase induction machine is carried out in the same assumptions as the actuation with the DC machine to highlight this has been compiled the global simulation scheme by coupling the model of the actuation system, operating at U/f constant and powered by a voltage inverter with the model of the ship. A single modification consisting in linking the required speed to propulsion, propeller with that supplied by the engine to achieve the speed of the march is required. The results obtained by simulation are similar to those from the DC motor actuation operating at constant flow. The speed of the ship increases slowly as a result of the weak load of the actuation engine through the durable torque produced by the propeller. The response time, to achieve the required speed, is virtually the same as the DC actuation

Given the similarity between the two types of actuations, it is proposed to introduce the speed adjustment of the ship in an outer loop by increasing the speed of the propelling over the nominal one, using the exiting resource. In this respect the output of the ship's speed regulator, which represents the speed force of the motor-propulsion group, shall be limited to the value of 204.1 rad/sec, i.e. an increase of about 30% above the nominal speed.

Analyzing the results of the simulation is found the same îmbunătațiri as the DC actuation results that the proposed solution is achievable and favorable. More acceleration duration and mechanical and electrical demands of the motor-propeller group can be easily altered and adapted to its needs and limitations.

The solutions analysed above have considered that the power supply of the electric motor a three-phase inverter of high power PWM voltage, produced in manufacturing. Another converter that could be used is the three-phase cycloconverter. A first advantage is provided by the reduced working frequency, 1-15 Hz, supplied by Cycloconverters which in conjunction with the adopted electric motor performs the small rotation speeds required for the propeller. In this idea a simulation was performed using the SIMULINK schematics and the engine adopted, with the limitation of the operating regime at steady U/f at the frequency of 15 Hz and, accordingly, a voltage of 1040 V. Also recalculated the transmission ratio of the gearbox to value i=7.28, and the new synchronism speed 47.124 rad/s. The simulation was carried out to accelerate the ship up to the marching speed. The main resulting sizes are shown below:

- The duration and form of acceleration shall not be altered as a result of being generated by the propeller;
- Strong torque charging is better sensitive, the availability of the engine is better exploited;
- The other characteristic sizes fall within the limits imposed by the engine.

It follows that the cycloconverter is constituted in a real source for the power of a three-phase induction motor-powered naval power supply.

# 7. CONTRIBUTION TO INCREASE ENERGY EFFICIENCY BY REDUCING THE ABNORMAL REGIME AND ABSORPTION OF REACTIVE POWER OF THE NAVAL SYSTEMS WITH DC MOTORS

## 7.1. INTRODUCTION

The use of adjustable electrical actuations with DC or three-phase induction machines for naval propulsion leads to some advantages in terms of conversion yield, managability flexibility and deeper driving automation As shown above. The need to achieve the adjustable character of the actuations involves the use of static converters as power sources [ION]. Depending on the engine used the sources can be:

- DC Engine: ac-dc converter with SCR Thyristors, controlled rectifier connected to the mains through an adaptation transformer;
- Induction Motor: three phase inverter voltage, connected to the mains through a diode rectifiers and an LC filter. There is a modern variant with a sinusoidal absorption PWM rectifier;
- Induction Engine: AC-ac converter, cycloconverter, with network connection through adaptive transformer.

Regardless of the variant used for the power supply, converters generate and inject into the current harmonic vessel network and absorb a significant reactive power. The ship's energy system, unlike

systems on land, is heavily influenced by the deflector regime generated by the converters. Thus decreases the availability in active power of the ship's generating system, increases power losses and voltage failures in the ship's network and decreases the overall yield of generation, transport and use of electricity.

## 7.2. AC-DC CONVERTER WITH SCR THYRISTORS. DISTORTING REGIME AND REACTIVE POWER

Two converters are used to achieve the proposed actuation scheme: The Statoric Converter, 310V and 30A; The Rotoric, 1000V, and 6915A converter. The stator converter has negligible power in relation to the Rotoric, which is why it will not be taken into account in the analysis of the deformant regime. At the rotors level the very high power, 6500 KW, indicates the use of a converter with 12 pulses. The converter is powered from the ship's network through a two-secondary transformer in the Ddy connection, for reasons of reducing the decomposed system injected into the network, being the most favorable scheme in this regard.

The actuation system was modeled in the space MATLAB-SIM POWER SYSTEMS., where the DC machine is an R + L + Em task. For the performance of the nominal operating system, the converter in the Rectier mode and the motor car, the order is adopted in the Rectier

$$\propto = 20^° \ (7.1)$$

That corresponds to the nominal engine voltage

$$U_N = 1000V \ (7.2)$$

Counter electric voltage

$$E_N = 970V \ (7.3)$$

Corresponds to the nominal speed and excitation. A well-filtered current is found following the provision of an additional inductivity Ld. Also, the rotoric voltage waves are those specific to the converter, and the switching angle is

$$\gamma = 5,2^° \ (7.4)$$

For starters, it analyzes the current absorbed by the transformer mayor. This current, Fig. 7.5, has a well-known form with a three-stage variation. It is chosen for spectral analysis, based on the rapid Fourier transform, FFT, three periods of the network tension in the stationary area of the electromagnetic regime, Fig. 7.5.

It makes the sinusoidal hypothesis of the three-phase power supply system, hypothesis very close to reality. The FFT provides the following electrical sizes:

- The fundamental current absorbed by the transformer at the frequency of 50 Hz,

$$I_1 = 1483A \ (7.5)$$

- Voltage-current dephase

$$\varphi = \alpha + \frac{\gamma}{2} = 22,6^° \ (7.6)$$

where α is the control angle of the rectifier;

- The distortant regime is characterized by

$$THD = 13,28\% \ (7.7)$$

Calculate the powers circulated in the system:

-DC power at the entry level of the electric motor

$$P_{cc} = V_d \cdot I_d = 1000V \cdot 6915A = 6915kW \quad (7.8)$$

- Active power absorbed by the transformer

$$P_T = 3 \cdot V_1 \cdot I_1 \cdot cos\varphi = 3 \cdot 1734 \cdot 1483 \cdot cos(22,6) = 7122,2kW \quad (7.9)$$

- Reactive power absorbed by the transformer

$$Q_T = 3 \cdot V_1 \cdot I_1 sin\varphi = 3 \cdot 1734 \cdot 1483 \cdot sin(22,6) = 3381,8kVAR \quad (7.10)$$

- Apparent power at the fundamental level

$$S_T = 3 \cdot V_1 \cdot I_1 = 3 \cdot 1734 \cdot 1483 = 7714,5kVA \quad (7.11)$$

- Power factor

$$cos\varphi = cos\left(\alpha + \frac{\gamma}{2}\right) = cos\, 22,6° = 0,923 \quad (7.12)$$

- The distorting residue

$$I_D = \frac{THD}{100} \cdot I_1 = \frac{13,28}{100} \cdot 1483 = 196,94A \quad (7.13)$$

- Actual value of the absorbed current

$$I_P = \sqrt{I_1^2 + I_D^2} = \sqrt{1483^2 + 196,94^2} = 1496A \quad (7.14)$$

- Total apparent power

$$S = 3 \cdot 1734 \cdot 1496 = 7782kVA \quad (7.15)$$

- Global power factor

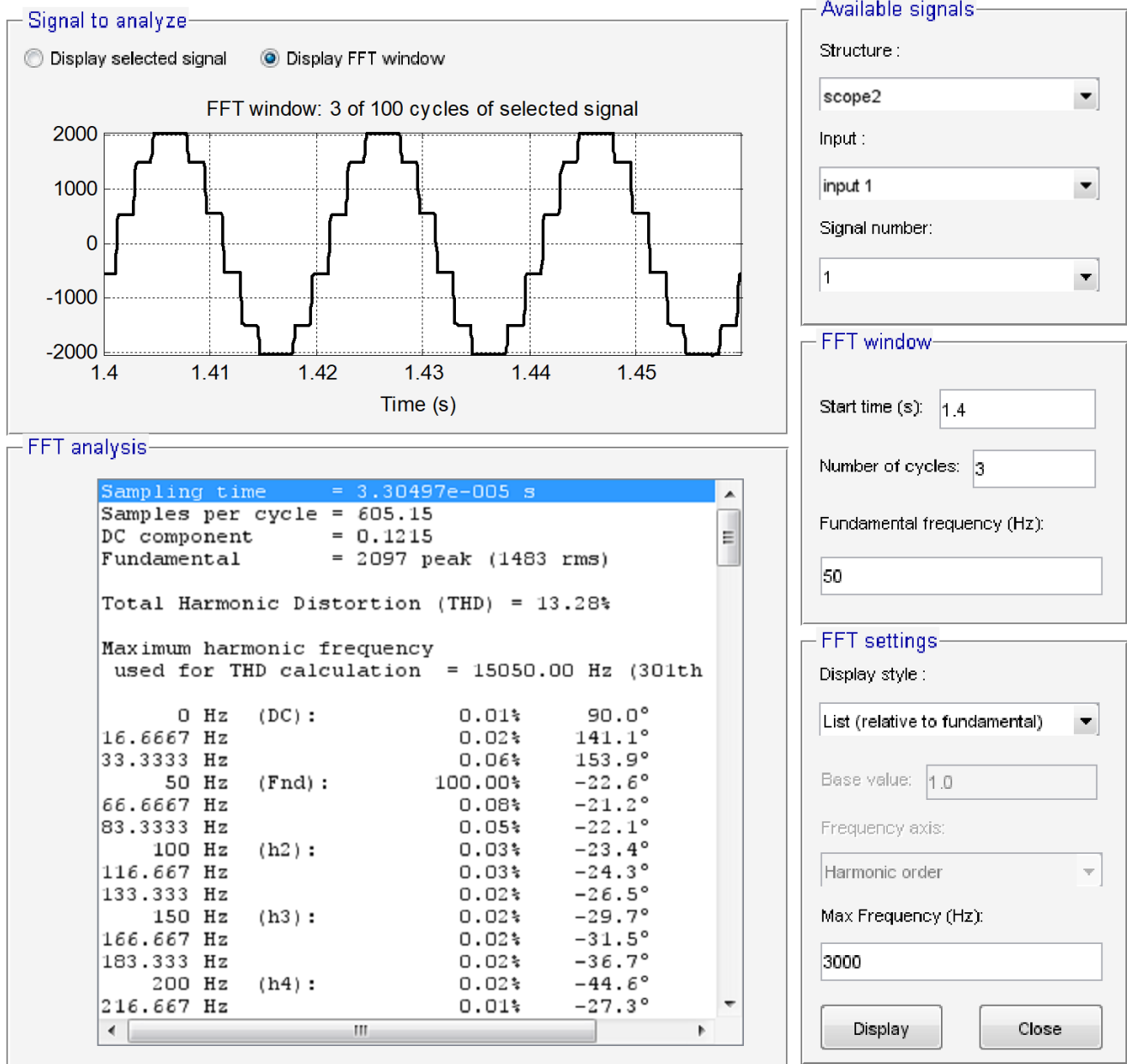$$k_P = \frac{P_T}{S_T} = \frac{7122,2}{7714,5} = 0,923 \quad (7.16)$$

Fig. 7.5 – Spectral analysis of the current absorbed from the grid.

Analyzing the results outlined above can conclude a fairly good behavior of the transformer assembly – converter. Thus, the power factor, (7.12) and the Global, (7.16), falls within the limits allowed in the energy networks on land. However, if the decomposition residue is reduced due to the transformer connection, the reactive power is consistent, especially as the angle of command used is favorable from this point of view. The same harmonic analysis is also carried out for the two secondary exits, in the triangle and in the star. Obviously, given the symmetry of the recovery scheme, the line sizes at the exit of the two secondary will be identical.

The two semi-secondary are directly affected by the conductive switch on one thyristor on another. This causes strong deformation of the tensions provided by the two semi-secondary, the and waveform presented for the second-in-the-star in Fig, 7.7.

Thus, for the line tension the distorting residue is

$$V_{DS} = \frac{THD}{100} \cdot V_S = \frac{11,93}{100} \cdot 403,6 = 48,15 \quad (7.26)$$

and the actual value of the power supply voltage of the converters becomes

$$V_{SM} = \sqrt{V_S^2 + V_{DS}^2} = \sqrt{403,6^2 + 48,15^2} = 406,5V \quad (7.27)$$

The total apparent power at the level of a semi-secondary is

$$S = \sqrt{3} \cdot V_{SM} \cdot I_{SM} = \sqrt{3} \cdot 406,5 \cdot 5628,8 = 3963kVA \quad (7.28)$$

Fig. 7.7. Voltage provided by the semi-secundaries.

Thus, for the line tension the distorting residue is

$$V_{DS} = \frac{THD}{100} \cdot V_S = \frac{11,93}{100} \cdot 403,6 = 48,15 \quad (7.26)$$

and the actual value of the power supply voltage of the converters becomes

$$V_{SM} = \sqrt{V_S^2 + V_{DS}^2} = \sqrt{403,6^2 + 48,15^2} = 406,5V \quad (7.27)$$

The total apparent power at the level of a semi-secondary is

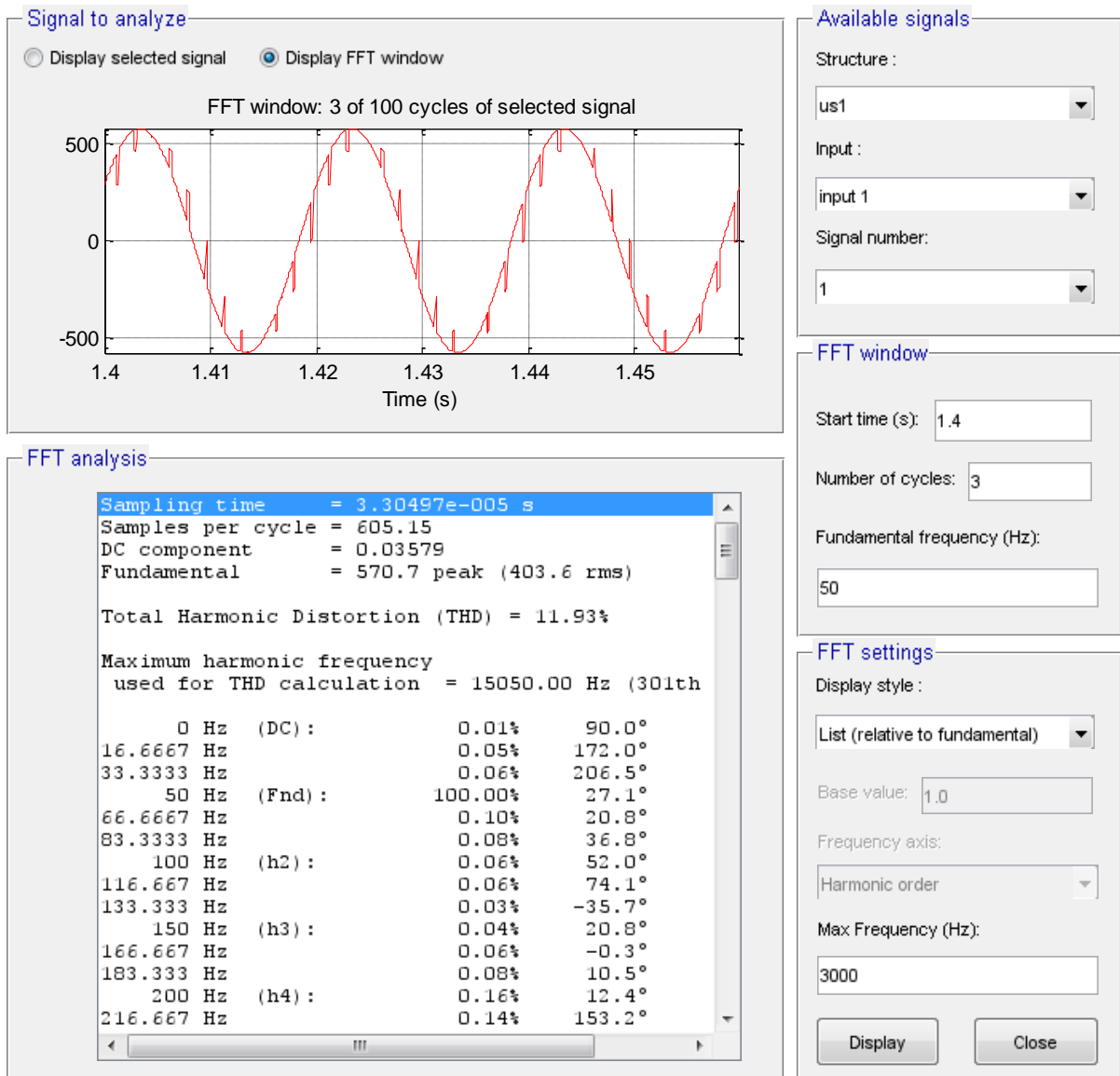$$S = \sqrt{3} \cdot V_{SM} \cdot I_{SM} = \sqrt{3} \cdot 406,5 \cdot 5628,8 = 3963kVA \quad (7.28)$$

## 7.3. REDUCTION OF DISTORTING REGIME AND REACTIVE POWER FOR A NAVAL DRIVE IN DC

### 7.3.1. DESIGN BASIS

It is proposed to compensate the distorting system and reactive power by connecting an active derivative filter with indirect control to the terminals of the primary winding of the power transformer, Fig. 7.10, where SD is the distorting load composed of the whole transformer, DC-AC converter with 12 pulses and actuation engine. As it is about compensating the current harmonics generated by the AC-DC converter It is made to the active filter structure of the derivative shown in Fig. 7.10 [AGA]. The ABC network is considered to provide a symmetrical three-phase system of voltage
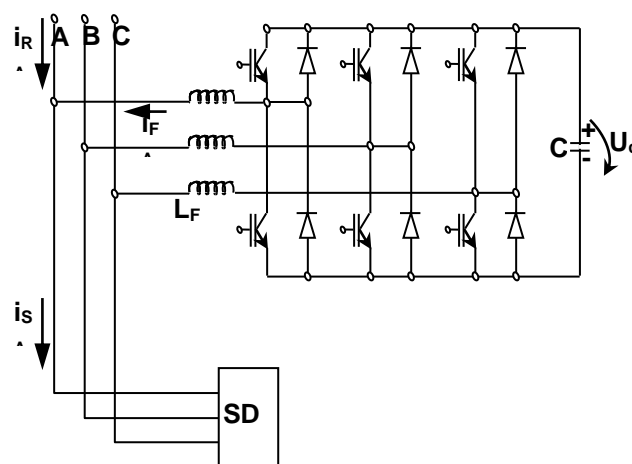


Fig. 7.10 – Active filtering principle scheme

On each phase of the assembly in Fig. 7.10 you can write the equations of the form

$$i_R(t) = i_S(t) - i_F(t) \ (7.32)$$

Where the three currents are in order: the current on a phase of the network, the distorting load and the active filter. The active filter's current

$$i_S(t) = i_{SP}(t) + i_{SQ}(t) + i_{SD}(t) \ (7.33)$$

i.e. an active component, a reactive one and another deformanta. From these three components only the first, the active one, can be absorbed from the network, while the other two must be supplied by the active filter. The latter still needs the absorption of an active power to keep the C capacity charged to the $U_C$ voltage, necessary for the operation of theactive filter converter. As a result, the current FA active filter will be

$$i_F(t) = i_{FP}(t) + i_{FD}(t) \ (7.34)$$

where $i_{FP}$ is the active component, and the $i_{FD}$ sums up the reactive and distorting components circulated by the FA. Imposing as $i_R(t)$ To be sinusoidal and in phase with the voltage of the network in (7.32), (7.33) and (7.34) results

$$i_R(t) = i_{SP}(t) - i_{FP}(t)$$
$$i_F(t) = i_{FP}(t) + i_{SQ}(t) + i_{SD}(t) \ (7.35)$$

The second equation (7.35) is essential for the problem formulated. From the perspective of the hard filter structure, Fig. 7.10, the derivation topology is best suited, in terms of its order things are much more complicated. In order to achieve the current $I_F(t)$, which in fact represents the imposition of the current which must provide the active filter, three steps are needed:

- Acquisition of data measured from the process, possible filtering and numerical processing;

- Spectral analysis consisting of determination of decomposition residue and reactive component for SD and FA currents;

- Elaboration of the control structure to carry out a real-time order and a null error tracking.

If the first stage does not raise particular problems, the second one requires remarkable difficulties. In order to achieve the spectral analysis of currents, at least a period of the signal is required obviously earlier. The spectral analysis itself requires a large amount of computing, which turns to another delay. Finally, the design and implementation of the order requires another time frame. It follows from the above reasons that it is not possible to achieve a null tracking error both in a steady state regime or especially in the dynamic one.

Currently there are a multitude of methods of controlling active filters [AGA], [GUR], [EPU1]. The most popular are: The method of instantaneous powers, the method of separating the deformist components, the method of symmetrical components and... All these methods are considering the most accurate and rapid determination of the decomposition spectrum, but the difficulties listed above are evident.

### 7.3.2. INDIRECT CONTROL METHOD

This control strategy intelligently uses the hardware components of the active filter, as well as the positioning of the transducers, so that the mathematical workings of the adjusting loops are minimal. [EPU1], [ROS].
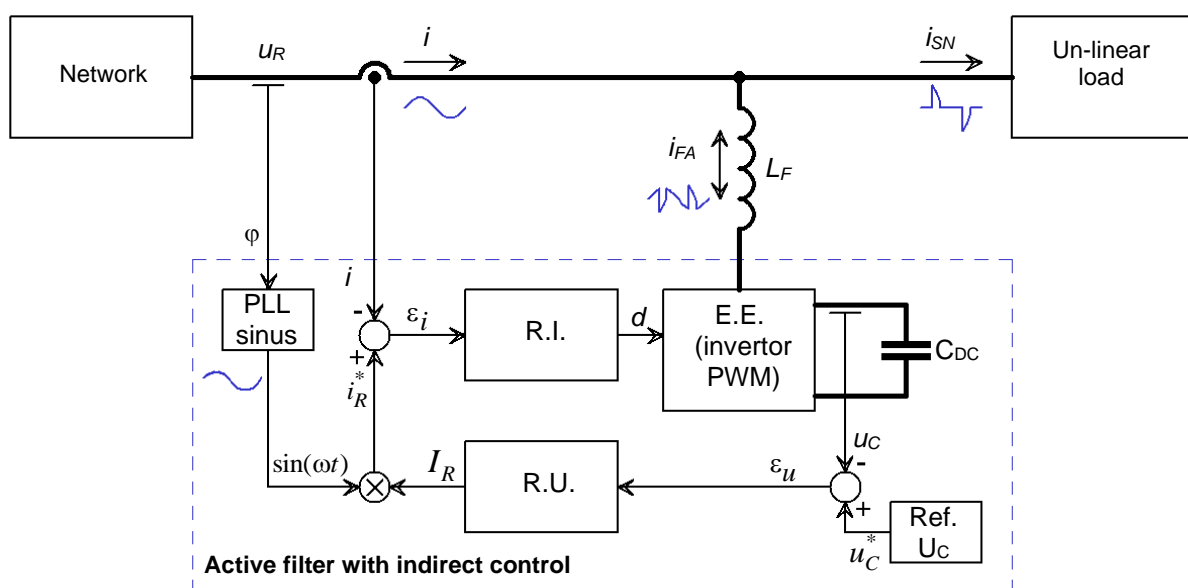


Fig. 7.11 – Structure of indirect control

Viewed as a whole, the active filter is a bidirectional AC/DC power converter that has to provide two functions:

- Constant retention of the output voltage $U_C$, measured at the terminals of the $C_{DC}$ condenator;

- current taken from the whole network distroting load – Active filter to be sinusoidal and in phase with the voltage of the mains.

To achieve these, the control structure in Fig. 7.11 is proposed. The structure consists of two cascading adjusting loops. In the outer adjustment loop, common for the three phases is controlled the continuous tension from the terminals of the $C_{DC}$ capacitor, the voltage to be kept constant. It must also have a sufficiently high value to avoid the entry of the voltage regulator RU in saturation and damage to the current RI adjustment loop. The current adjusting loop is the inner loop, with its own regulator on each phase. The current loop on a phase is of an imposing size

$$i_R^*(t) = i_R \cdot sin(\omega t + \Phi_R) \ (7.36)$$

where $I_R$ is the peak value of the current required, and $\varphi_R$ the initial phase of the mains voltage. From (7.35) it follows the need to purchase the three-phase system of tensions and the separation of the initial phase. This is physically achievable through a PLL loop or by more advanced methods [EPU]. The task to be compensated by the active filter is connected after the active filter current transducer, so the sum of the two currents is measured. In this way, the consumer becomes a disturbance affecting the two adjusting loops of the active filter. The principle of negative reaction, after which both adjusting loops operate ensures the rejection of the disturbance as long as none of the system components has entered the limitation.

In the common connection point, the equation (7.31) can be written in the form

$$i_R(t) = i_S(t) + i_F(t) \ (7.37)$$

Because the current supplied by the filter does not have a single defined meaning. Break down the currents in (7.36) and group the foundations of currents after

$$i_R(t) = i_{S1}(t) + i_{F1}(t) + i(t) \ (7.38)$$

where $i_{S1}$ and $i_{F1}$ are the fundamentals and,

$$i(t) = i_F(t) + \sum_k i_{SK}(t) + i_{SQ}(t) \ (7.39)$$

It is the sum of the harmonics generated by the active filter, harmonics absorbed by the deformante load and the reactive component. As the current adjustment loop absorbed from the mains imposes the sinusoidal and phase-in shape with its tension, it follows that all the different components of the fundamental are cancelled. Determining the correct amplitude of the current network, so that the energy stored in the filter condense keeps constant from one period to the next, is made on the basis of the difference between the required voltage and the actual voltage at the capacitor terminals. This results in the reference signal for the current regulator

$$i_R^*(t) = \varepsilon_u \cdot \frac{u_R}{\sqrt{2} \cdot U_R} = \varepsilon_u \cdot sin(\omega t) \ 7.40$$

where $\varepsilon_u$ is the output of the voltage regulator.

As noted, the method requires minimal mathematical calculations, easy to implement both analog circuits and numerical circuits. The performance will be directly dependent on the quality of the sinus

signal used, so in order to obtain a harmonic distortion factor as low as possible for the adjusted current, it is necessary to use a PLL loop to remake the sinusoidal network voltage form.

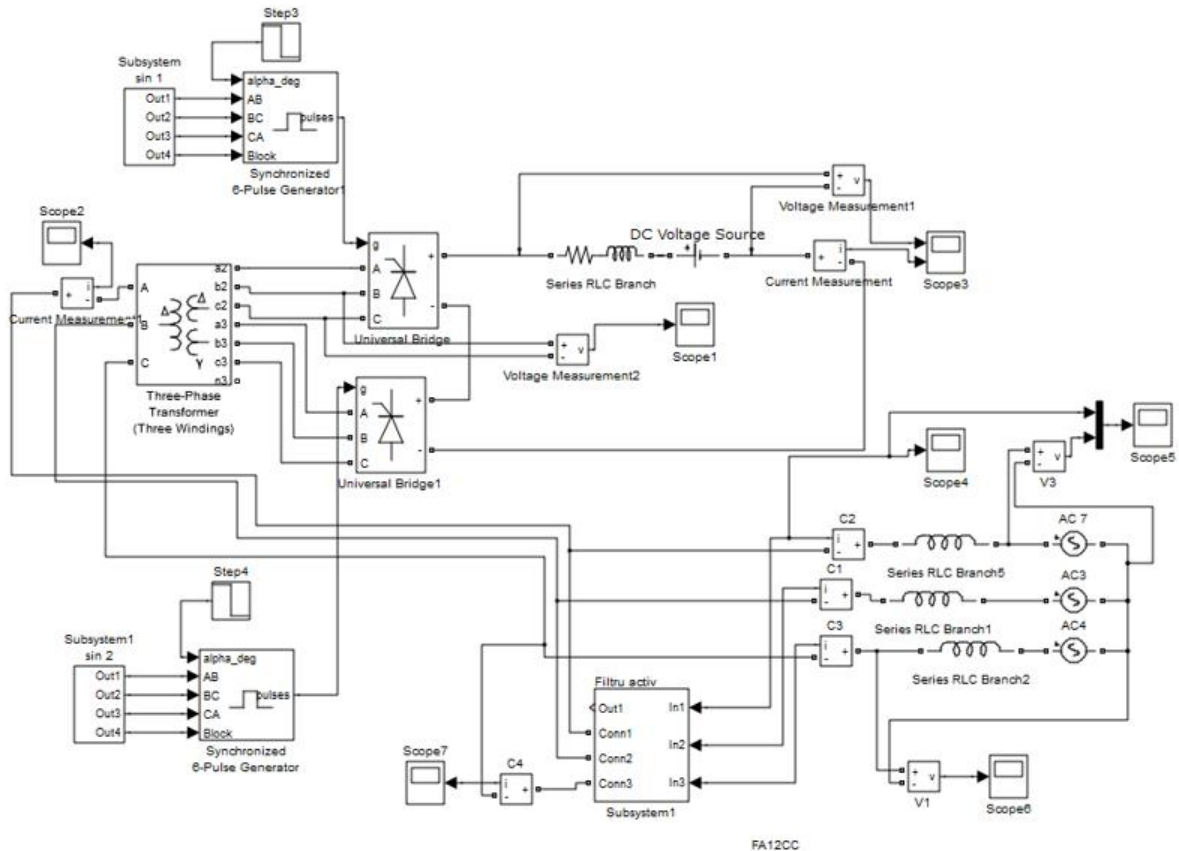## 7.3 VALIDATION BY NUMERICAL SIMULATION OF ACTIVE FILTERING IN THE TRANSFORMER PRIMARY



Fig. 7.12 – SimPower Systems Simulation Scheme for active filtering in transformer primary

With a view to validating the active filtration solution in the transformer mayor, the simulation scheme of the inverter's schema and the control resulting in a new model was completed. shown in Fig. 7.12. The simulation was performed for a start at rest until the nominal stationary regime was reached, lasting from 0.15 seconds to 1.2 seconds.
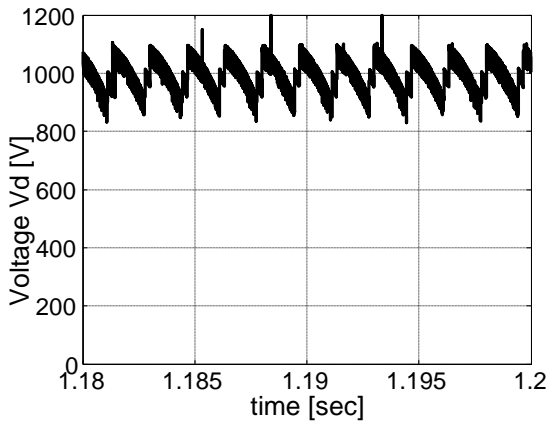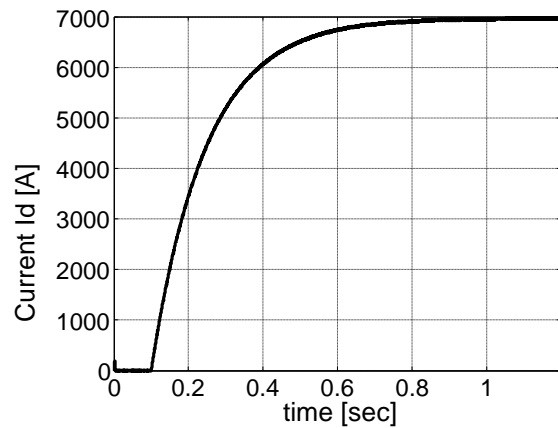
Fig. 7.15 – Rotor voltage
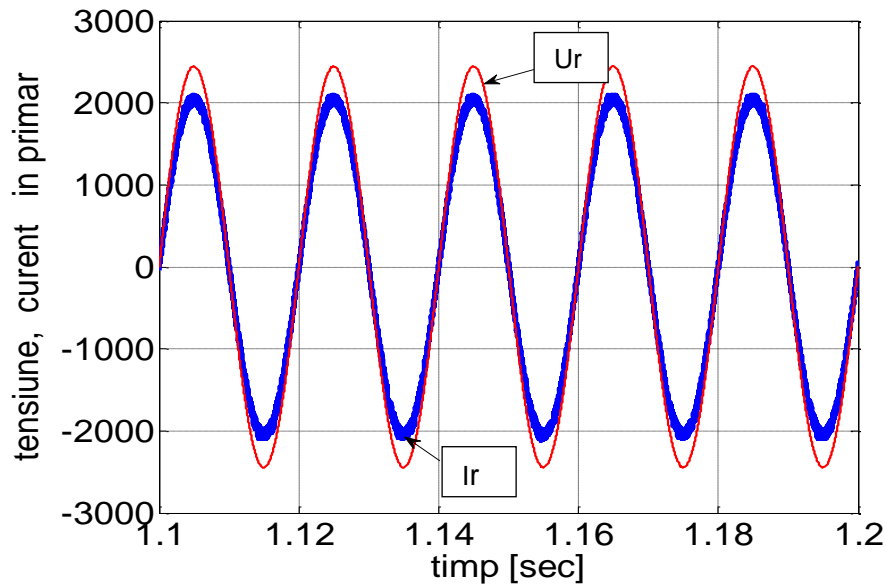


Fig. 7.16 – Rotor Current



Fig. 7.17 – Voltage and current absorbed from the mains

In Fig. 7.15 and 7.16, the forms of variation of the voltage and the Rotoric current are presented. The rotors current is identical to that of the non-filter operation, indicating that the load, actuation, is not affected by the presence of the filter. With regard to the rotoric tension pulses, they contain a high frequency that practically modulates natural pulses. This modulation is due to the switch in the active filter, which produces multiple harmonics of the frequency of switching.

The sinusoidal form and the null defuse are found in relation to the voltage on the mains of this current. There are some deviations from the sinusoid, all of the high frequency, generated by the switching of the converter and the principle of modulation used, with hysteresis, as well as regulating currents with regulators, also with hysteresis. Deviations from sinusoid fall into the Histesis band adopted for the current regulators.

For qualitative appreciation of the effect of using the active filter, the spectral analysis was performed according to the above method. The results obtained are contained in Fig. 7.18.
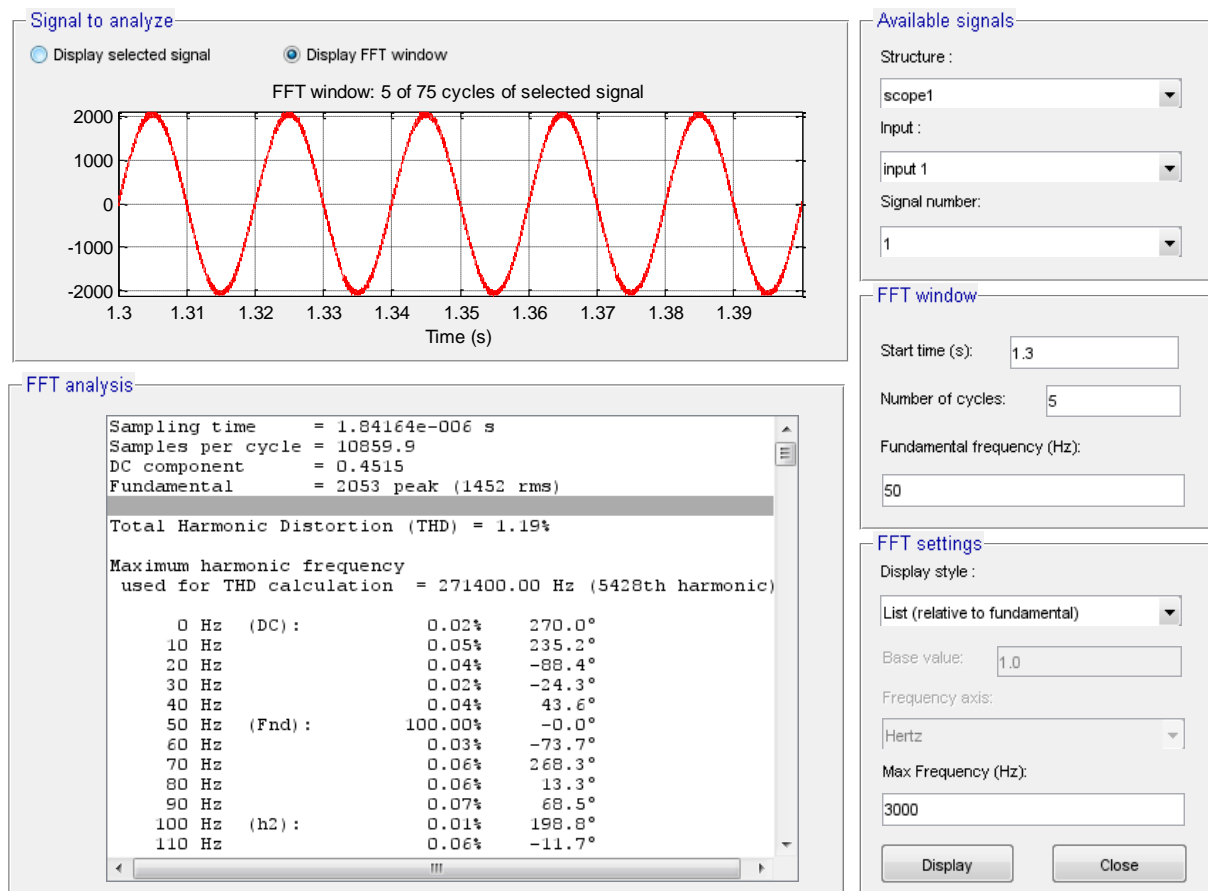


Fig. 7.18 – Spectral analysis of absorbed current

5 periods of supply voltage placed in the stationary regime area were chosen for analysis. The sizes that interest have values:

   -The actual value of the foundation, $I_1$= 1452a;

   -THD [%] = 1.19%;

   -Initial phase of current φ = 0.

The very small THD leads to virtually null deform power, and the same initial phase for tension and current cancels reactive power. In these conditions we can calculate the apparent power of the transformer after

$$S_T = 3 \cdot V_1 \cdot I_1 = 3 \cdot 1734 \cdot 1452 = 7553,3 kVA \quad (7.59)$$

Comparing this power to the original results in a difference

$$\Delta S_T = 7714,5 - 7553,3 = 161,2 kVA \quad (7.60)$$

Which represents about 2.1%. There is also a decrease in the current absorbed, approx. 31 A, which leads to reducing power losses in the converter and through the power lines.

Finally, there remains a problem to investigate, namely that of active filter behavior in dynamic mode. For this it was analyzed the variation of THD and current phase-tension for an important variation of the rotoric Current, Fig. 7.23, the dynamic regime occurring between 0.8 and 1.5 seconds.
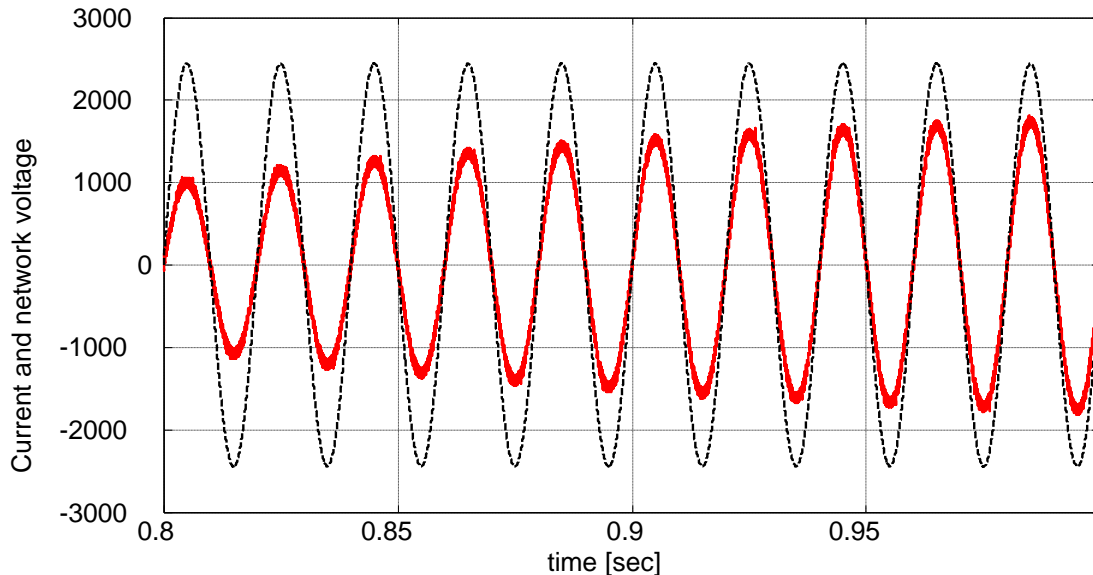


Fig. 7.23 – Dynamic network current and voltage

A first assessment can be made on Fig. 7.23 relative to the variation shape of the current absorbed from the mains: The current is sinus and in phase with the supply voltage. The second way consisted in the calculation for 5 periods of the two characteristic sizes for the operation of the active filter: THD and current phase-tension, table 7.1.

Table 7.1

| Interval [sec] | .8-.9 | .9-1.0 | 1-1.1 | 1.1-1.2 | 1.2-1.3 | 1.3-1.4 | 1.4-1.5 |
|---|---|---|---|---|---|---|---|
| THD [%] | 2,34 | 1,91 | 1,78 | 1,48 | 1,48 | 1.35 | 1,36 |
| Φ [grade] | -0,4 | -0,1 | -0,1 | 0,0 | 0,0 | 0,0 | 0,0 |

In Table 7.1. the following conclusions shall be found:

- The THD grows insignificant at the beginning of the dynamic regime, after which it decreases asymptotically to the steady-state value;

- The variation of voltage phase angle – current is insignificant, being in the margin of error.

## 7.4. VALIDATION BY NUMERICAL SIMULATION OF ACTIVE FILTERING IN SECONDARIES OF THE TRANSFORMER

Another possibility for reducing the depressive regime consists in placing each secondary of an active derivative filter, compensating for the depressive regime produced by each bridge rectifier in part. At first glance, three advantages are seen:

- Lower working voltage for the filter inverter as a result of the lower supply voltage of the two decks with thyristors;

- Lower power for each filter, approx. 50%, from the power of the primary filter;

- Avoidance of transfer by transformer of superior harmonics and reactive component with proper shrinking of power losses in the system.

To analyse the proposal, the model in Fig. 7.2 is used. Operating at nominal parameters, the converters being controlled at $\alpha = 20°$, load, engine current being 6915A.

The spectral analysis for the current absorbed by the transformer mayor is further carried out. The results obtained in the two cases, active filter in primary and secondary, are presented in table 7.2.

Tabelul 7.2

| Active filter | $I_P$ | THD | ø | Observations |
|---|---|---|---|---|
| Primary | 1452 A | 1,19 % | 0 grade | Un-noticeable switching |
| Secondary | 1445 A | 5,19 % | 0,4 grade | Noticeable switching |

CThese two functions are slightly different, the use of the active filter in the primary is more favourable: the smaller THD, basically the switches are not found on the network and the current absorbed is virtually the same.

# 8. CONTRIBUTION TO INCREASING ENERGY EFFICIENCY BY REDUCING THE DISTORTING REGIME AND ABSORPTION OF REACTIVE POWER OF NAVAL ELECTRIC PROPULSION SYSTEMS WITH INDUCTION MOTORS

## 8.1. INTRODUCTION

For naval propulsion with AC, induction or synchronous motors, the available power supplies are: three-phase inverters of high power voltage, cycloconverters, or, in the particular case of the use of synchronous machine, the current inverter with Extinguishing from the load. If in the case of inverters the interaction with the network is not direct but through a rectiizer and a filter, the Cycloconverter is a network converter, so with the injection of deforming regime and reactive power absorption. Furthermore, the propeller drive with the three-phase induction machineand the Cycloconverter is favourable from punct de vto the realization of reduced speeds required by propellers and simplification Engine mechanical transmission – propeller. For these reasons it was adopted to analyse the energy efficiency of the conversion of the Cycloconverter system – three phase induction motor.

## 8.2. AC-AC CYCLOCONVERTER WITH SCR THYRISTORS. DISTORTANT REGIME AND REACTIVE POWER

The power of the three-phase induction motor for propulsion is adopted from a cycloconverter based on the AC-DC converter with 6 pulses in three-phase bridge, Fig. 3.9. The Cycloconverter is also equipped with movement currents and $L_K$ inductivity to limit them. In terms of availability at the output of the cycloconverter they are:

- Output Voltage: 250 – 3750V;

- Output Frequency: 1 – 15Hz;

- Rated current: 725A;

- Maximum current: 1450A;

- Inductivity limiting movement currents $L_K$: 0, 02H;

- Sinusoidal command.

As regards the engine, in order to avoid an ineffective scheme and simulation time, it was replaced by an R + L load with the parameters:

- R=4,198 ohms;

- L=0,0248H.

These adopted values shall ensure the nominal current above and the power factor, also

Nominal. In Fig. 8. 3. The simulation scheme of the. Control subsystem and force on a phase of the cycloconverter shall be presented. The scheme was drawn up in the light of the following:

- The conversion scheme is proposed in the variant with movement currents and L K inductivity to limit them.

- As far as the order was chosen for the sinusoidal, as a result of the command structure in SimPower Systems, which has as input the angle α.

From the point of view of operation, two aspects are concerned:

- Achieving voltage and current parameters at the output of the converter as well as their quality;

- The interaction of the network converter, the dedeformant regime and the absorption of reactive power.
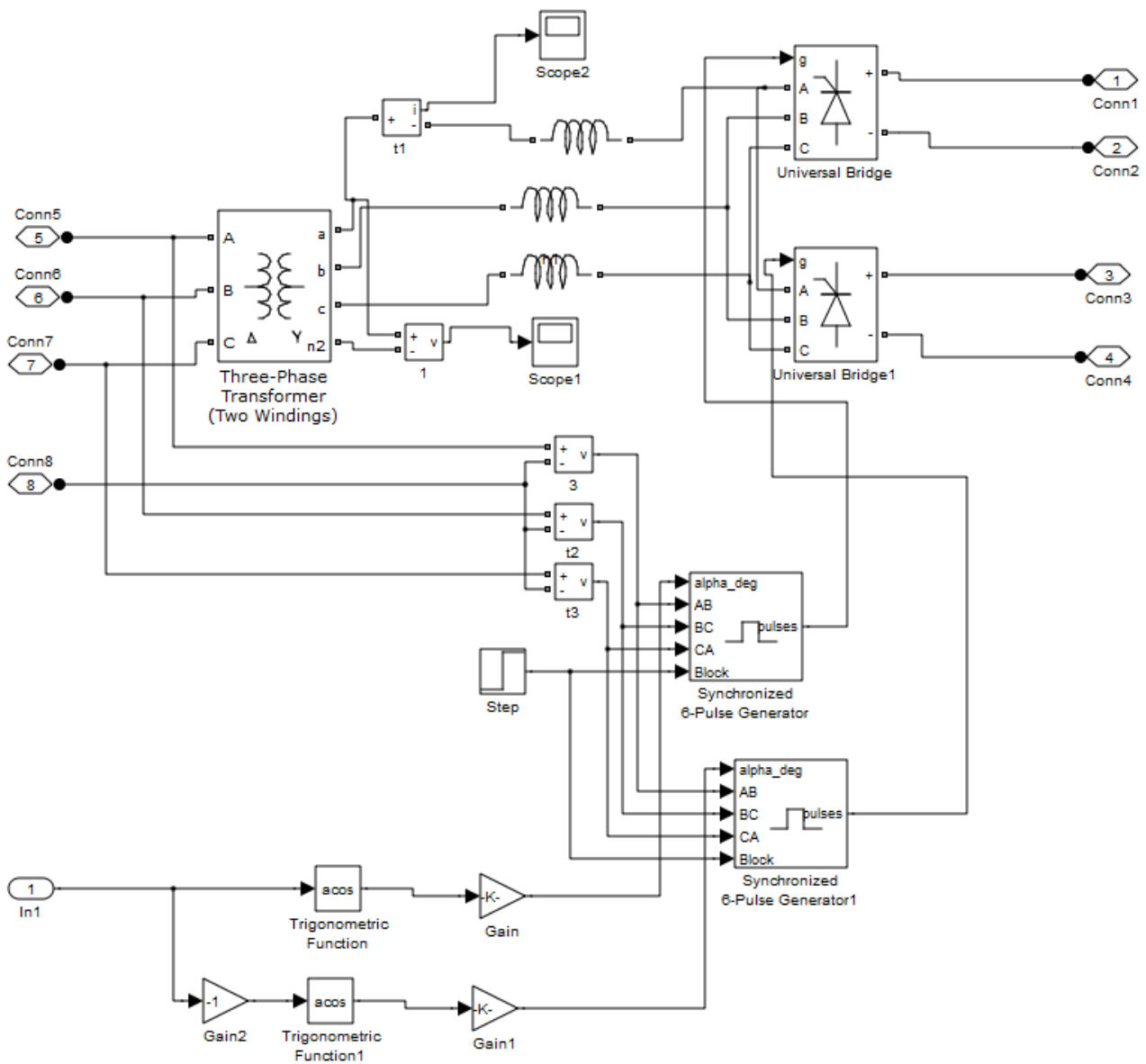
Fig. 8.3 – The control and force subsystem on a phase of the Cycloconverter

The performance of the functional parameters at the output of the Cycloconverter is presented synthetically in table 8.1. For four different operating frequencies, in compliance with the report, at the command level, U/f = constant. In table 8.1 The main output sizes of the cycloconverter, so the load feeding, are: the actual values of the fundamentals of phase voltage, $U_s$, phase Current, $I_s$, and related THD's; Current – voltage phase angle; The apparent, active and reactive powers provided.

Table 8.1

| $f_S$ [Hz] | $U_c$ [V] | $U_S$ [V] | $THD_U$ [%] | $I_S$ [A] | $THD_I$ [%] | Phase angle, $\varphi$ | S [kVA] | P [kW] | Q [kVAR] |
|---|---|---|---|---|---|---|---|---|---|
| 15 | 0,81 | 3685 | 20,41 | 766,7 | 1,65 | 29,2 | 8475 | 8366 | 4135 |
| 10 | 0,54 | 2646 | 31,33 | 591 | 2,85 | 20,3 | 4691 | 4400 | 1627 |
| 5 | 0,27 | 1413 | 72,29 | 331 | 6,2 | 10,5 | 1403 | 1379 | 255,7 |
| 1 | 0,054 | 313,3 | 184,5 | 74,4 | 8,32 | 2,1 | 69,99 | 69,9 | 2,56 |

In Fig. 8.8. 8.9, 8.12, 8.13. The waveforms for the voltage and phase current are presented for frequencies of 10 and 1 Hz.

The following comments are required:

- The output voltage form is heavily deformed and the THD is virtually unacceptable;

- The current waveform is almost sinusoidal, and the very small THD, at acceptable level.;

- Tension-voltage-current as well as active and reactive powers correspond to the simulated operation regime;

- In relation to the lowering of the output frequency, it is found to be worsening of the dedeformation regime, increase of the voltage and output current THD, but also an improvement of the power factor;
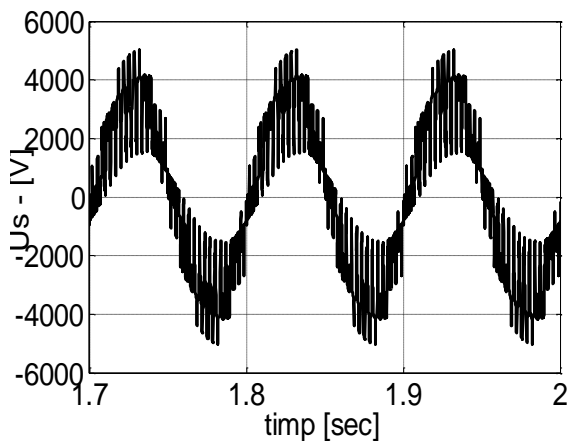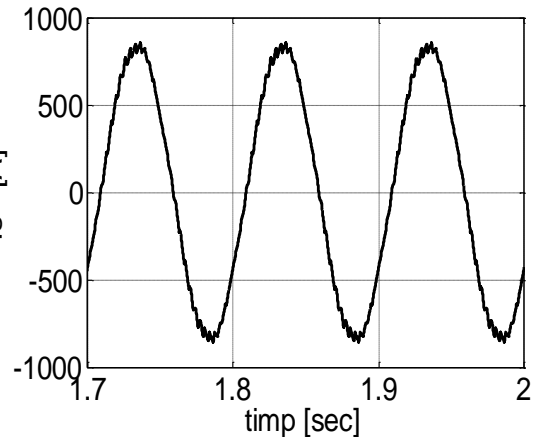


Fig. 8.8 – $U_S$ 10Hz



Fig. 8.9 – $I_S$ 10Hz
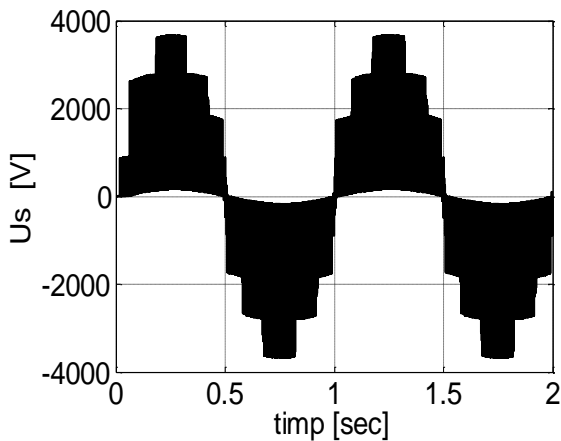
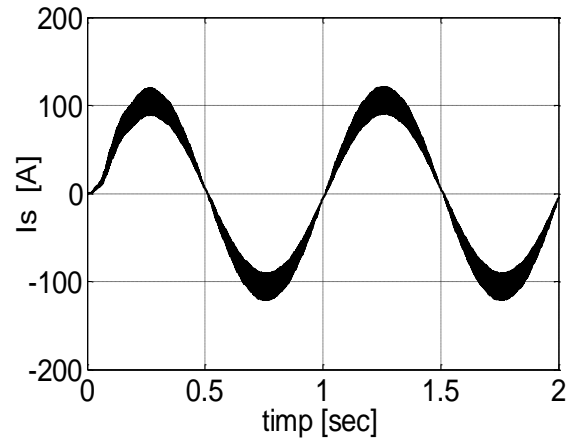Fig. 8.12 – U$_S$ – 1Hz                                                    Fig. 8.13 – I$_S$ 1Hz

It follows from the above analysis that it is not necessary, in the pregnancy, to further reduce the deformity regime and absorbed reactive power. The R + L character of the load as well as the presence of limitations on the limitation of movement currents shall ensure good filtration of the current provided to the load.

With regard to the influence of the Cycloconverter in the supply network, for the same simulations above, further analysis of the current absorbed from the mains, I$_D$, its THD, voltage-current phase angle φ, active component I$_W$, and reactive I$_Q$ and distorted, I$_R$, absorbed current as well as appropriate powers. The results are presented synthetically in table 8.2, and in Fig. 8.14 − 8.17 Waveforms for network voltage, U$_D$, presumed to be sinusoidal, and phase current absorbed, I$_D$

Table 8.2

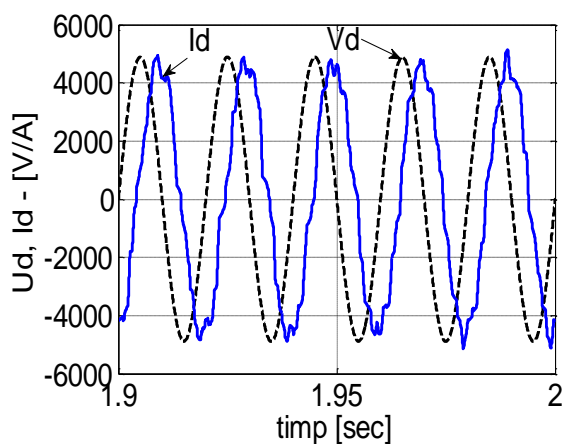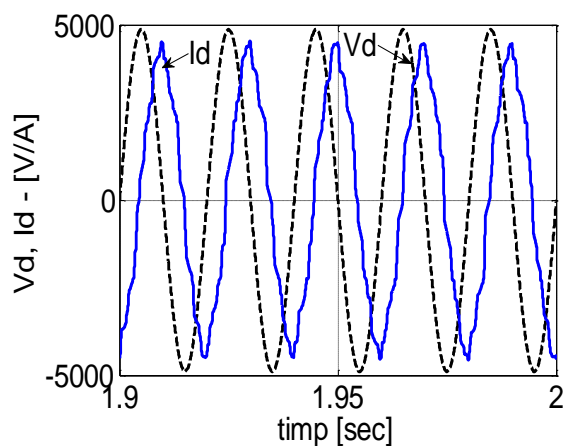| f$_c$ [Hz] | U$_c$ [V] | U$_d$ [V] | I$_d$ [A] | THD$_I$ [%] | Phase angle $\boldsymbol{\varphi}^o$ | I$_W$ [A] | I$_Q$ [A] | I$_R$ [A] | S [kVA] | P [kW] | Q [kVAR] |
|---|---|---|---|---|---|---|---|---|---|---|---|
| 15 | 0,81 | 3458 | 3307 | 5,56 | 77,3 | 727 | 3226 | 166,6 | 38454 | 8454 | 37513 |
| 10 | 0,54 | 3458 | 2997 | 5,9 | 81,8 | 427 | 2966 | 176,8 | 31088 | 4434 | 30770 |
| 5 | 0,27 | 3458 | 1696 | 20,1 | 85,2 | 141,9 | 1680 | 340,9 | 17613 | 1473 | 17522 |
| 1 | 0,054 | 3458 | 587,3 | 36,7 | 88,5 | 15,4 | 587 | 215,5 | 6093 | 159,5 | 6091 |

Fig. 8.14 – $U_d$, $I_d$ at 15Hz
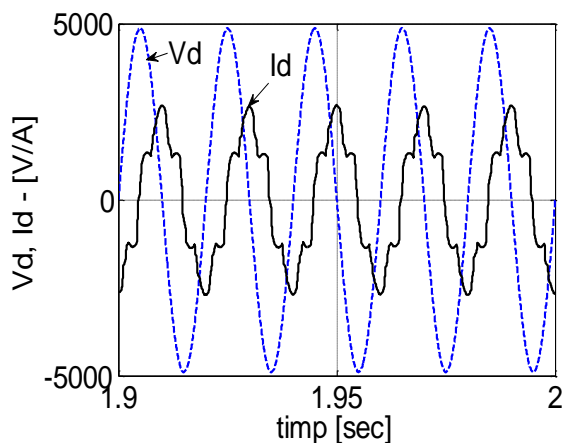


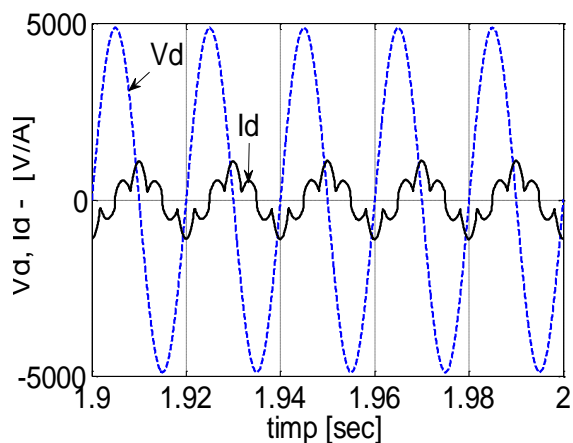Fig. 8.15 – $U_d$, $I_d$ at 10Hz



Fig. 8.16 – $U_d$,$I_d$ at 5Hz



Fig. 8.17 – $U_d$, $I_d$ at 1Hz

The analysis of the absorbed current leads to the following conclusions:

-The deforming system injected into the network is relatively low, the deflating component of the current increasing with the decrease of the output frequency, when the THD becomes unacceptable, the Deformante component becoming comparable or higher than the active one.

-The reactive current component is appreciable, the voltage-current is about $70 - 85$ degrees, and the extremely low power factor, between 0.225 and 0.0226. Reactive power has an appreciable value, being required by variable control of the converter decks and traffic currents.

-It is absolutely necessary to ensure the provision of means for reducing reactive and deformante components.

## 8.5. REDUCTION OF DISTORTION AND REACTIVE POWER FOR AN AC NAVAL ACTUATION WITH CYCLOCONVERTER

The solution for the compensation of reactive power and reduction of the deformist is obviously the one used in the case of DC propulsion, active filter with indirect control. There are also two variants of the active filter location: In the transformer mayor or one active filter in each secondary. The second variant requires three-phase active filters with independent control which makes the solution economically inelegible right from the start. Therefore, the active filter solution located in the transformer mayor after the DC model is still viable.

The filter implementation implies, as in DC. Sizing the filter and carrying out the control structure. For the proper operation of the active filter must be dimensioned, as in DC,: the $U_C$ voltage of the $C_{DC}$ capacitor for energy accumulation; inductivities $L_F$ on the active filter output. The calculation of the active filter parameters shall be drawn up for the nominal load operation of the actuation system and follow the DC methodology resulting in the required values.

- Voltage on storage capacity

$$U_C > \sqrt{2} \cdot \sqrt{3} \cdot U_d = \sqrt{2} \cdot \sqrt{3} \cdot 3458 = 8435 \quad (8.10)$$

where Ud It's the phase voltage of the supply. Unanimously it is accepted that the $U_C$ be as large as possible, which is why the

$$U_C = 10000V \quad (8.11)$$

- $L_F$ inductivity must accumulate sufficient energy to retrieve the highest current gradient of the load

$$L_F \leq \frac{U_C}{\Delta I /_{\Delta t}} = \frac{10000 \cdot 0,002}{2550} = 0,00784H \quad (8.12)$$

.

In view of the existence in the coupling circuit and the own inductivity of the rectifying decks, the

$$L_F = 0,2mH \quad (8.14)$$

The accumulation capacity shall be calculated for energy considerations necessary to be supplied by the active filter for the compensation of the decomposed and reagent product of the load and cycloconverter. Thus, at the nominal operation the transformer absorbs from the grid, at the fundamental level, a current

$$I_D = 3307A \quad (8.15)$$

Under a

$$THD = 5,56\% \quad (8.16)$$

The current distorted residue is

$$I_R = I_D \cdot THD = 3307 \cdot 0,056 = 185,9A \quad (8.17)$$

Reactive component is

$$I_Q = 3226A \quad (8.18)$$

A variation of the voltage on the storage capacitor is accepted during this interval

$$\Delta U_C = U_{CM} - U_{cm} = 10500 - 9500 = 1000V \quad (8.20)$$

U$_{cm}$, respectively u$_{cm}$ , are the maximum and minimum tensions, admitted on the capacitor.

The power circulated by the filter for the compensation of the decompression regime and the reactive component, for the most unfavourable situation, 15Hz, table 8.2, is the date of

$$S_{FA} = \sqrt{3} \cdot U_d \cdot \sqrt{I_Q^2 + I_R^2} = \sqrt{3} \cdot 3458 \cdot \sqrt{3226^2 + 166{,}6^2} = 19324746VA \quad (8.21)$$

This power is made available by the active filter capacity on account of the energy stored in the form

$$W_C = \frac{1}{2} \cdot C \cdot U_C^2 \quad (8.22)$$

The power

$$P_C = \frac{dW_C}{dt} = C \cdot U_C \cdot \frac{\Delta U_C}{t_C} \quad (8.23)$$

Equalizing (8.21) with (8.23) results

$$C = \frac{S_{FA} \cdot t_C}{U_C \cdot \Delta U_C} = 0{,}0064F \quad (8.24)$$

The value is adopted (8.24), which will cover the entire adjusting range, 1Hz – 15Hz, the power of the filter, S$_{FA}$ , decreasing with the decrease in the output frequency, table 8.2

## 8.5.  VALIDATION BY NUMERICAL SIMULATION OF THE ACTIVE FILTERING SOLUTION

For the validation of the proposed solution, the structure of the models from C. C. was used, preserving the structure of the indirect control system, used in DC propulsion and recalculating the parameters of the voltage and current regulators.

Simulated load assembly, Cycloconverter and active filter for operation at 4 output frequencies, 15, 10, 5 and 1 Hz over a time interval of one second, leaving the initial null state and connecting to the network at zero time. In Fig. 8.20 – 8.23 the waveforms for the Vd supply voltage, considered sinusoidal, and the current absorbed Id are presented, and in table 8.3 a synthesis of the main electric sizes.
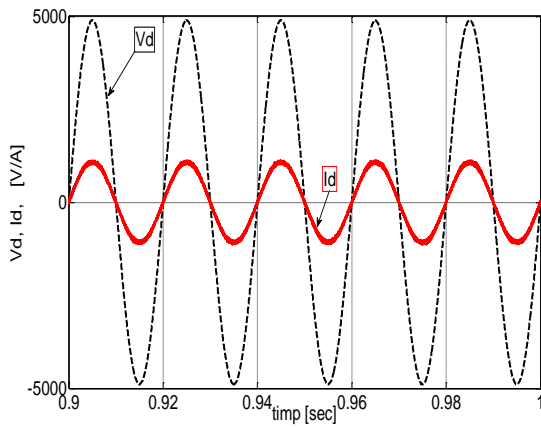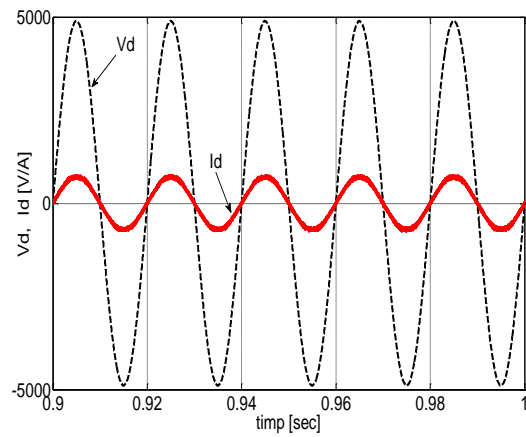
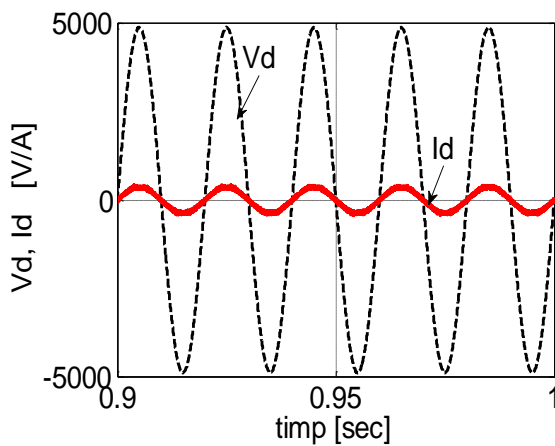Fig. 8.20 – V_d, I_d at 15Hz



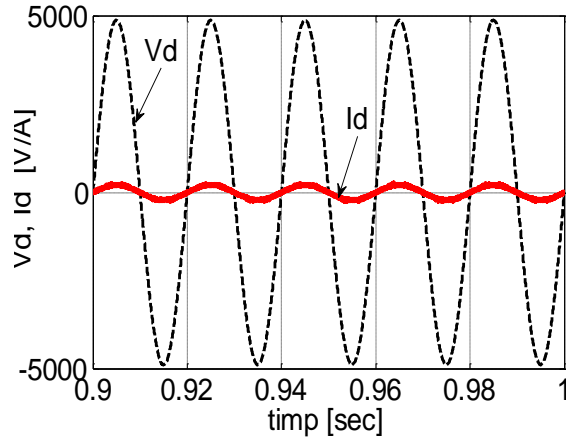Fig. 8.21 – V_d, I_d at 10Hz



Fig. 8.22 – V_d, I_d at 5Hz



Fig. 8.23 – V_d, I_d at 1Hz

Graph analysis leads to the following conclusions:

- The absorbed current Id decreases consistently with the natural operation without active filter, table 8.2. Thus, at an output frequency of 15Hz the current absorbed decreases from 3307 A to 765.15 A, and at 5Hz from 1696A to 261, 06A;

- The current shape is sinusoidal and in phase with the supply voltage, the reactive component of the current being null, and the deform component also decreases, the THD dropping from 2.01% for 15 Hz to 10.29% for 1Hz;

Table 8.3

| $f_c$ [Hz] | $U_c$ [V] | $U_d$ [V] | $I_d$ [A] | $THD_I$ [%] | Phase angle $\varphi^o$ | $I_W$ [A] | $I_Q$ [A] | $I_R$ [A] |
|------|------|------|--------|-------|-----|-------|------|-------|
| 15 | 0,81 | 3458 | 765,15 | 2,01 | 0 | 765 | 0 | 15,37 |
| 10 | 0,54 | 3458 | 502,73 | 3,04 | 0 | 502,5 | 0 | 15,27 |
| 5 | 0,27 | 3458 | 261.06 | 5,85 | 0 | 260,6 | 0 | 15,24 |
| 1 | 0,054 | 3458 | 153,4 | 10,29 | 0 | 152,6 | 0 | 15,70 |

- The growth trend of THD is preserved with decreasing the output frequency of the cycloconverter. More in Table 8.3 It is found that the actual value of the Deformist component is virtually constant relative to the output frequency.

- The active filter introduced is very effective, the apparent power circulated between the source and the load reducing substantially, table 8.4. Diminishing the apparent powers is achieved by decreasing the circulated currents. The effects are evident: decreasing the nominal power of the transformer, lower rated current power semiconductors, power loss in reduced sensitive circuit elements;

Table 8.4

| | Apparent power [kVA] | | | |
|---|---|---|---|---|
| Frequency | 15Hz | 10hz | 5Hz | 1Hz |
| No active filter | 38.454 | 31.088 | 17.613 | 6.093 |
| With Active filter | 7.936 | 5.215 | 2.708 | 1.591 |

The proposed energy efficiency solution is real, gives remarkable properties to the Cycloconverter system – three-phase induction machine.

-The dynamic performance analysed for the situation of a network coupling of the assembly are not characterizing because the operating system is not a frequent one. Much more interesting is the modification of the task as the system already operates in a stationary regime. Thus in Fig. 8.29.se shows the variation in the current load, Is, at a modification, doubling, load R + L, at time t = 0.6 seconds, previously the system being in steady state regime. The time constant of the load circuit being very small change in the current load is virtually instantaneous. A change, also instantaneous, of the initial phase of the current is also found as a result of changes in the load impedance. What is of interest is the variation of current absorbed from the network, Id, whose developments are shown in Fig. 8.30. There is a certain increase in the current, less than on pregnancy, keeping the initial phase unchanged and entering the new stationary regime after a time interval equal to 3 semiperiods, so after about 30 milliseconds what is very performant [BIM].
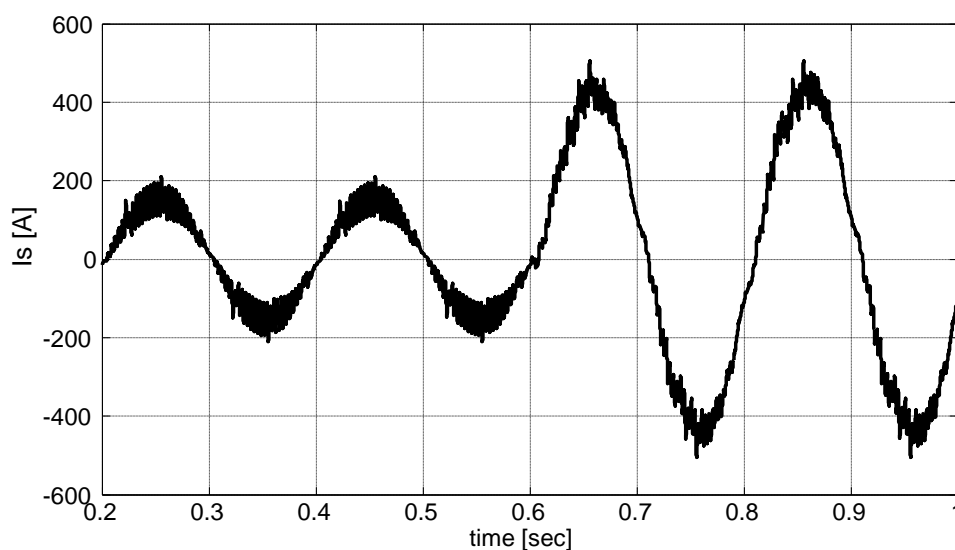


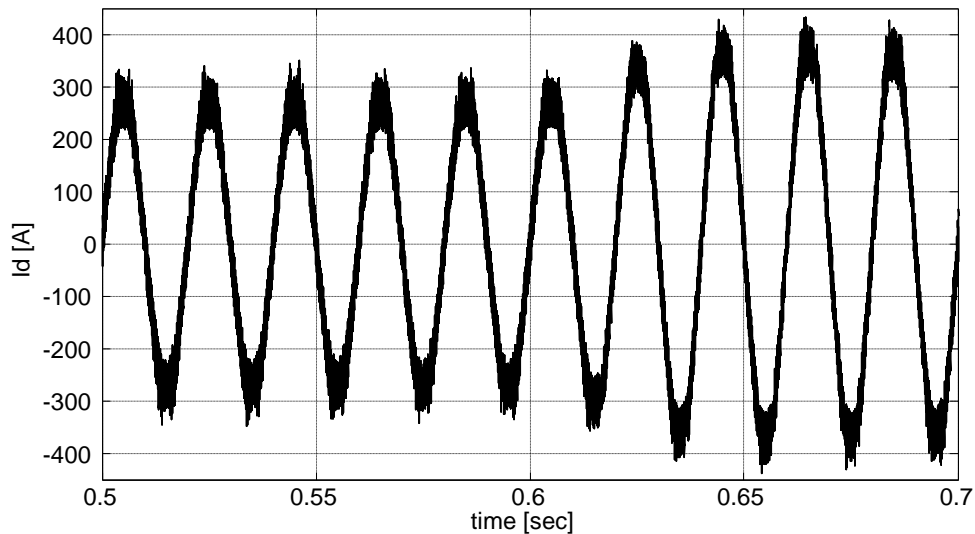Fig. 8.29 – Current variation I$_S$ to load change

Fig. 8.30 – Current variation I$_d$ to load change

In conclusion, the solution developed in the work is of good energy performance, acting, regardless of frequency, as a linear and active consumer, by a unit power factor. Static and dynamic performance are also remarkable, the active indirect control filter offing the deforming and reactive powers, practically in real time.

# 9. FINAL CONCLUSIONS AND CONTRIBUTIONS

## 9.1. GENERAL CONCLUSIONS

The propulsion of ships requires, in principle, two basic requirements: ensuring the prescribed speed of the ship's marching and minimizing fuel consumption. The use of a Diesel engine, very widespread, raises two problems: linking the marching speed with the reduced engine speed beach at which the minimum fuel consumption is achieved, requiring even a mechanical reducer; Use the adjustable, CPP propeller to increase the optimum required speed.

Electric propulsion in fact an adjustable electrical actuation system, avoids the problems outlined above as a result of several possibilities for adjusting electrical parameters, voltage, current, and mechanics, speed, torque. On the other hand, new problems arise regarding the management of the electrical powers circulated between the ship's energy system, finite capacity, and the propulsion drive powered by a static converter of appreciable power and generator of serious harmonics and reactive regimes.

From the multitude of electric motor pairs – usable converter for propulsion were adopted for analysis the ones with one-step conversion being the most economical: DC motor – Network Converter with SCR thyristors; Three-phase induction motor – Cycloconverter. Both, steady state and dynamic regimes, have been taken into consideration for different reasons. Dynamic regimes, accelerating the ship at the speed of marching or stopping, have an insignificant duration relative to the march itself, so from energy point of view is irrelevant. Instead, the steady state regimes, the ship goes to marching speed are decisive for the system's energy load balance. Dynamic models, including

automatic control, have been designed to study the dynamic behaviour of the ship, the effectiveness of the control designed and the acquisition of various marching gear levels.

The purpose of the analysis consisted in increasing the efficiency of the use of electricity and optimising the nominal parameters of the equipment composing the system, transformers, converters, Motors.If the active power generated by the converter is strictly determined by the strong torque of the propeller finding itself in the power grid, reactive and distorted power depends on the configuration and performance of the equipment used and also power charging. The two powers, unhelpful, but absorbed from the network from other conditions, have well-known effects:

- Limiting the active power produced by the generators of the ship's energy system, as a result of loading with reactive current and dedeformant;
- Increased power losses in equipment and networks;
- OverPower of system equipment.

It follows the need to assess the reactive and deforming powers, their size and variation depending on the operating regime and the design of the solutions for the cancellation or, if it is not possible to compensate the total, minimize them. In order to achieve this, it is necessary, obviously, to build high-performance models that describe the system's operating regimes as accurately as possible.

The vessel itself and the propellers are difficult to shape as a result of the presence in the hydrodynamic characteristics of the system, established by experimental or theoretical methods, of non-linear relationships between dependent coefficients as a condition size Propelling and dynamic and cinemics. All parameters and, implicitly, all stationary regime sizes can be evaluated. This way you can completely define any stationary operation. Switching to a dynamic model, necessary to assess the dynamics of the ship, is difficult to achieve as a result of the variation of the ship's default characteristics. Using the data provided by the ship builder, resulting from the tank samples and the projecting of the propeller, a powerful dynamic model was made, which describes with a good approximation of the ship's behavior. The models, stationary and dynamic, were numerically simulated, stationary operating points found on the features provided by the dynamic model, which confirms the quality of the dynamically designed model. In the final part of Chapter 4, the use of CPP and FPP in the case of electric propulsion shall be analysed, resulting in the conclusion: the required propellers are the one with fixed pitch, FPP.

In chapter 5, DC engine propulsion and AC-DC network Converter with SCR Thyristors are developed with 12 pulses. For the actual actuation, the classic model with constant and variable flow and Shema of control, also classical, with cascade adjustment of electrical and mechanical parameters in the order of time constants was adopted. The model has been simulated numerically offering full satisfaction. In the next phase it was coupled to the model ship, through the dynamic model shown above. A very high duration is found to accelerate the ship from rest to nominal marching speed. On the other hand, a poor engine load is noted, generated by the evolution of the propelling torque. An original control scheme, called the ship speed control, is proposed, by adding an external adjustment loop of the ship's speed, duly granted. There is a substantial reduction in acceleration time and a higher net load of the engine, in the process, in certain situations, diminishing the flow. On the other

hand, the thruster is overrequested in speed during the final acceleration period. In this DC engine propulsion It is perfectly achievable with the achievement of remarkable perfomanses.

In Chapter 6, the electric propulsion with three-phase induction motor and cycloconverter develops. The d/q model is performed with the orientation of the rotors magnetic field and the control on two independent channels, flow and torque, the engine can work at U/f = Const. and u=Const., f=var. The model has been simulated numerically for various dynamic regimes offering Full satisfaction. Coupling this model with that of the ship leads to the same conclusions as the DC actuation and here The outer loop of the speed adjustment of the ship is inserted the results being the same. Conclusion: AC Motor Propulsion It is perfectly achievable with the achievement of remarkable perfomanses. It should also be noted that at the same power the gauge of the three-phase induction motor is less sensitive than the DC engine, which is very advantageous for loading and better use of ship's premises.

The last two chapters, 7 and 8, contain most of the original developments in terms of efienticing the power flows circulated by electric propulsion. So for DC propulsion, carried out with a network converter with 12 pulses and D/dy transformer, as the most favorable configuration for both the load and the network, the harmonic and reactive components of the current absorbed by the The mayor and the two secudation. With regard to the size of the reactive component the decisive role has the phase command and the switch, the power factor being variable but acceptable as a value to the nominal operation. As for the dedeformant regime injected by the network converter He is consistent, far above the permissible 3% value of THDului. The defragmentation regime is more pronounced in the two semicundation versus the primary due to the filter effect of the transformer. And the task of the converter, type E + R + L, has a filter role reducing the deforming regime with the increase in the load current. The analysis indicates the need to provision the conversion system with a strategy for the reduction or cancellation of the two components. Being variable as value the only applicable solution is the active parallel type power filter, placed either in the processor's mayor or two fuses on the two semisecundare. Applying a performance control strategy, called indirect control, was obtained the cancellation of the reactive current component, reduction of the harmonic regime, THD = 1.19% and reducing the power of the transformer and converter. In conclusion, active, physically achievable filtering is very favourable by significantly reducing the powers circulated on the ship.

A similar procedure was used for AC actuation with cycloconverters. For reasons of reducing the size of the network transformer, the three-phase bridge configuration, with circulation currents and 3-secondary transformer, was adopted. The analysis of the power flows indicates a highly absorbed reactive power and a variable but relatively low deforming regime, the deflecting component of the current increasing with the decrease of the output frequency, when the THD becomes unacceptable, the component Comparable or higher than the active one.

In conclusion, the provision of an active power filter in the mayor of the network transformer is very favourable, significantly reducing the power of the network transformer, the reactive regime and the network-injected harmonics.

In conclusion, it can be said that research developed in the work is important and devoted to certain energy efficiency issues on board Cargou ships. The results of the research can be easily implemented, favorable effects, reduction of the dedeformation regime, cancellation of reacive power

and reduction of equipment gauge, being important, accessible from costs and maintenance point of view. Moreover, the control method used, the indirect command, allows the global approach of the ship's energy system, using a FAP bar form factor with the propulsion Drive converter, the highest power receiver, and another FAP system for the other sum.

## 9.2. CONTRIBUTIONS

The work of the proposed research involved the necessity of formulating and solving complex naval problems, but also from the area of static converters, adjustable elctrium actuation systems and automatic control. The following contributions shall be claimed as original:

1. Carrying out the vessel model for dynamic regimes;

2. Analysis of the electrical propulsion with CPP and FPP with the selection of FPP solution;

3. Designing a sinusoidal control solution for cycloconverters;

4. Construction of individual SIMULINK models for: vessel, network converters and propulsion actuation systems;

5. The achievement of the overall models of the two configurations selected for the energy analysis, with the network Converter with SCR and with the Cycloconverter;

6. Structuring and calculating the automatic control for the two configurations above;

7. Introducing a new concept for automatic control, adjusting the speed of the ship, improving engine load and reducing the duration of dynamic regimes.

8. Analysis of reactive and dedeformative regimes for the two configurations;

9. Choice of FAP topology to compensate the power factor and THD;

10. Calculation method for CPC connection elements;

11. Graphic material obtained by simulation, interpretation of results and findings;

12. Conclusions on the implementation of the proposed solutions.

## 9.3. PUBLISHED WORKS

[1] **G. Frangopol**, C. Dache, A Solution for Reducing Harmonic Regime and Reactive Power Absorbed by a Cycloconvertor. Proceedings ISEEE 2019 Galati;

[2] **G. Frangopol** ,C. Dache, A Dynamic Model for an Electric Cargo Ship. Proceedings ISEEE 2019 Galati;

[3] Cristinel Radu DACHE,  Emil ROȘU,  Marian GĂICEANU, Teodor DUMITRIU, Romeo PĂDURARU, Traian MUNTEANU, **Gabriel Frangopol - Linearized model of the variable flux induction motor drive** - Proceedings of the 2016 International Conference and Exposition on Electrical and Power Engineering (EPE 2016), Book Series: International Conference and Exposition on Electrical and Power Engineering, Pages: 658-663, ISBN:978-1-5090-6128-0, ISSN: 2471-6855, WOS:000390706300131;

[4] Cristinel Radu Dache ; Emil Mina Rosu ; Marian Gaiceanu ; Romeo Paduraru ; Traian Munteanu ; **Gabriel Frangopol - Practical results on asynchronous motor optimal control in field weakening regime** - Publication Year: 2017, Page(s):1 – 5, 2017 5th International Symposium on

## 9.4. Works published in journals BDI indexed

**[5]** Cristinel Radu DACHE, Emil ROȘU, Marian GĂICEANU, Romeo PĂDURARU, Traian MUNTEANU, **Gabriel FRANGOPOL - Flux weakening Optimal Control of theThree-Phase Induction Motor** - The Scientific Bulletin of Electrical Engineering G.

## 9.5. FUTURE DEVELOPMENTS

The results obtained in the work indicate that the solution of using an FAP with indirect control solves the problem of reactive and dedeformative regimes for electric propulsion systems. We believe it follows the validation of the solution on a real case, a pilot propulsion. Overall compensation could also be studied at the level of the Cargo ship's power plant.